AMERICAN UNIVERSITY OF BEIRUT

THE USE OF GEOGRID REINFORCEMENT FOR ENHANCING THE PERFORMANCE OF CONCRETE OVERLAYS

by
HAYSSAM MOHAMAD ITANI

A thesis
submitted in partial fulfillment of the requirements
for the degree of Master of Engineering
to the Department of Civil and Environmental Engineering
of the Faculty of Engineering and Architecture
at the American University of Beirut

Beirut, Lebanon
February 2016

AMERICAN UNIVERSITY OF BEIRUT

THE USE OF GEOGRID REINFORCEMENT FOR ENHANCING THE PERFORMANCE OF CONCRETE OVERLAYS

by
HAYSSAM MOHAMAD ITANI

Approved by:

_____   Advisor
Dr. George Saad, Assistant Professor
Civil and Environmental Engineering Department

_____   Co-Advisor
Dr. Ghassan Chehab, Associate Professor
Civil and Environmental Engineering Department

_____   Member of Committee
Dr. Samir Mustapha, Assistant Professor
Mechanical Engineering Department

Date of thesis defense: February 5, 2016

AMERICAN UNIVERSITY OF BEIRUT

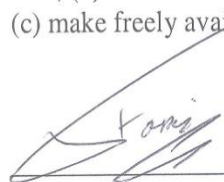# THESIS, DISSERTATION, PROJECT RELEASE FORM

Student Name: __Itani_____Hayssam_____Mohamad__
                             Last   First   Middle

☑ Master's Thesis   ◯ Master's Project   ◯ Doctoral Dissertation

☑   I authorize the American University of Beirut to: (a) reproduce hard or electronic copies of my thesis, dissertation, or project; (b) include such copies in the archives and digital repositories of the University; and (c) make freely available such copies to third parties for research or educational purposes.

☐   I authorize the American University of Beirut, **three years after the date of submitting my thesis, dissertation, or project,** to: (a) reproduce hard or electronic copies of it; (b) include such copies in the archives and digital repositories of the University; and (c) make freely available such copies to third parties for research or educational purposes.

_____   18 / 2 / 2016

Signature   Date

This form is signed when submitting the thesis, dissertation, or project to the University Libraries

ACKNOWLEDGEMENTS

AN ABSTRACT OF THE THESIS OF

Hayssam Mohamad Itani   for   Master of Engineering
                                              Major: Structural and Materials Engineering

Title: The Use of Geogrid Reinforcement for Enhancing the Performance of Concrete
       Overlays

The objective of this research is to assess the feasibility of the use of geogrid as main reinforcement in thin concrete members such as overlays to enhance their performance by providing additional tensile strength and ductility. More importantly, the aim is to study the ability of geogrid to control crack propagation and mitigate reflective cracking. For that reason, experimental setups were prepared to assess and quantify the effect of inclusion of the geogrid in Portland cement concrete overlays under mode I cracking. The experiments comprise of two tests: the direct tension test and the flexure test. These two tests are conducted on plain concrete samples and reinforced concrete with one layer of uniaxial geogrid. On the other hand, finite element mathematical models were developed using ADINA to simulate the performance of the prepared specimens. These models are also calibrated with experimental results for later investigation and sensitivity analysis. Results of testing confirm the geogrid reinforcement enhances the performance of the concrete overlay in terms of post-cracking behavior, crack mouth opening displacement and mode of failure.

CONTENTS

ILLUSTRATIONS

TABLES

I dedicate this work to my beloved mother

CHAPTER 1

INTRODUCTION

1.1 Problem Statement

Placing a structural concrete overlay atop existing pavements is a conventional pavement rehabilitation method. This type of maintenance is considered cost-effective and can be used for almost any combination of existing pavement type and condition, desired service life and anticipated traffic loading. Concrete overlays are widely used because they offer many benefits, including increased load carrying capacity, extended service life, fast construction and low maintenance requirements (Taylor, et al., 2007).

However, reflective cracking in the new overlay has been a serious challenge associated with pavement rehabilitation. Reflective cracking involves the development of cracks in the new overlay that mirror the cracks and/or joints in the old existing pavement. Traffic loading and environmental effects are the primary external causes of reflective cracking.

When these cracks reflect to the surface over time, they can cause surface roughness and deterioration; also they allow water penetration to the underlying subgrade which can lead to further pavement distress. Eventually, the pavement becomes a shattered slab that requires replacement which can be costly Therefore, reflective cracks have to be monitored and maintained. Transverse cracking is a key measure of concrete pavement performance for jointed plain concrete pavements. These cracks occur perpendicular to the centerline of

the pavement and they are generally caused by thermally induced shrinkage at low temperatures when the tensile stress due to shrinkage exceeds the tensile strength of the concrete.

No solution for the complete prevention of reflective cracking has yet been suggested by researchers due to the number of variables that are involved in the nature of this cracking (Khodaii & Fallah, 2009). Therefore, delaying the crack propagation is the best solution adopted so far. The incorporation of geosynthetic materials in the design of paved and unpaved road systems has been shown to enhance the performance and extend the service life of pavements (Khodaii & Fallah, 2009). A geogrid in the concrete overlay may help delay and reduce reflective cracking by providing reinforcement and strain-relief. It is necessary to investigate reinforcing mechanisms of the geogrids for mitigating crack propagation. Quantification of the effect of geogrids will provide better understanding of its effectiveness and offer an opportunity to identify important factors that affect its reinforcing performance.

1.2 Objective

The major objective of this project is to evaluate and quantify the effectiveness of using geogrids in thin concrete overlays to mitigate reflective cracking. By studying the effects of this inclusion on the behavior of thin concrete members subjected to mode I fracture which is caused by external wheel load and temperature variations.

Geogrids are known to possess favorable characteristics in terms of strength, ductility and ease of installation. Tasks conducted throughout the course of this project will provide a better understanding of the mechanisms behind the reinforcing performance and important factors influencing it. Behavioral aspects of geogrid-reinforced concrete overlays to be evaluated include maximum load capacity, load-deflection response, crack mouth opening, crack propagation rate, flexural strength, and mode of failure.

The methodology of this project is divided into parts: experimental and analytical. For the experimental part, new test setups, like direct tension test and flexure test, were developed to study the behavior of geogrid as reinforcement. As for the analytical part, a finite element software "ADINA" is selected for the analysis. The FE models were validated by the data obtained from the experimental testing. These models will be used for later investigation on the topic.

1.3 Organization of thesis

This thesis is organized into five chapters. Chapter 2 provides a literature review of the topic, describing the problems related with the use of thin concrete overlays and their modes of failure; it also presents a review on the use of geosynthetics in various fields of civil engineering. Chapter 3 provides an introduction, description, results and analysis of the first performed test (Direct tension test) which assesses the use of geogrid in thin concrete member subjected to mode-I cracking due to thermal loading. Chapter 4 provides an introduction, description, results and analysis of the second performed test (flexure test)

which assesses the use of geogrid in thin concrete member subjected to mode-I cracking due to wheel loading. Chapters 3 & 4 also include finite element models development and validation of the performed tests. The fifth and final chapter presents the summary of the major conclusions and recommendations for further research in this area.

CHAPTER 2

LITERATURE REVIEW

2.1 Concrete Overlays: definition, usage, classification and advantages

One of the most used techniques for maintenance and rehabilitation for concrete and asphalt pavements is the use of concrete overlays. This type of maintenance is considered cost-effective and can be used for almost any combination of existing pavement type and condition, desired service life and anticipated traffic loading. Concrete overlays are widely used because they offer many benefits, including increased load carrying capacity, extended service life, fast construction and low maintenance requirements (Taylor, et al., 2007). Concrete overlays are classified according to the existing pavement type and the bonding condition between layers (Smith, et al., 2002). They can be either bonded or unbonded concrete overlays.

Overlays that are bonded to an existing pavement creating a monolithic structure are considered bonded concrete overlays. To use that type, the existing concrete pavement should be in good structural condition and the existing asphalt pavement should be in fair condition. Unbonded concrete overlays add structural capacity to the existing pavement, they are considered as new pavement constructed on a stable base. There is no bond between the overlay and the underlying pavement (Taylor, et al., 2007). Both overlays can be placed on existing concrete pavements, asphalt pavements or composite pavements.

Bonded concrete overlay is a thin concrete layer bonded to an existing concrete pavement; its thickness is typically from 2 to 5 in. It is used to increase the structural capacity of an existing concrete pavement or to improve its overall ride quality, skid resistance and reflectivity (Taylor, et al., 2007). Bonded overlays are used only where the underlying surface is free of structural distress and relatively in good condition; otherwise the cracks will reflect from the deteriorated surface to the new pavement. To achieve full bond, it is required to prepare the surface of the existing pavement by cold milling, sandblasting or waterblasting, this process will remove all oil, grease, paint and surface contaminants (Huang, 1993).

As for unbonded concrete overlays, a separation layer exists between the new concrete layer and the existing concrete pavement, this separation layer is typically 1 in thick of hot mix asphalt. It is placed to provide a shear plane that helps preventing cracks from reflecting up from the existing pavement into the new overlay (Taylor, et al., 2007). Furthermore, the separation layer prevents the interlocking between the two concrete surfaces so that both are free to move independently. These types of overlays are typically thicker than the bonded ones, ranging from 4 to 11in thick. The existing concrete pavement could be in any condition due to the existence of the separation layer which prevents reflective cracking. However, overlays on pavements in advanced stages of deterioration should be considered cautiously, because expansive materials-related distresses can cause cracking in the new overlay (Taylor, et al., 2007).

For deteriorated concrete pavement, asphalt concrete (AC) overlays has been considered as a typical rehabilitation method due to their fast construction; however,

multiple forms of early distress accompanied with the use of AC overlays such as reflective cracking, pothole and rutting which may occur as a result of the different physical characteristics between the AC overlay and the existing concrete pavement (Kim & Lee, 2013). Because of the similarity in material properties, bonded concrete overlays have been recently assessed as a viable alternative. In addition, concrete overlays can serve as cost effective maintenance and durable rehabilitation solution (Harrington, et al., 2007).

2.2 Cracking of Concrete

Concrete cracking strength is the tensile strength of concrete subjected to pure tension stress (Kim & Taha, 2014). This strength is quantified through several types of tests; the most common between them are the direct tension test, the modulus of rupture test and the splitting test (Zheng, et al., 2001). The occurrence of cracks in concrete elements is evaluated by the tensile strength and tensile strain capacity of concrete; the maximum concrete can hold without forming a continuous crack is the maximum tensile strain of concrete (Swaddiwudhiponga, et al., 2003).

2.3 Fracture mechanics

Three fracture modes were presented in the report done by (Al-Qadi, et al., 2008); a cracked pavement system can be loaded in any one or a combination of the three modes. (Figure 2-1)

7

1- Mode I (Opening mode) results from thermal and traffic loading that are applied normally to the crack plane

2- Mode II (Sliding mode) results from traffic loading causing in-plane shear loading

3- Mode III (Tearing mode) results from out-of-plane shear loading

(Ruiz, et al., 2001) Reported that the failure of Portland cement concrete in Mode II requires greater stress than that required in Mode I because of the aggregates interlocking along the crack plane. Therefore, Mode I parameters can be the critical criteria to enable crack propagation through the material (Kim, 2007). The tearing mode (Mode III) occurs when out of plane shearing load is applied. This causes sliding of the crack faces parallel to the crack leading edge. This mode of loading may occur only if the plane of the crack is not normal to the direction of the traffic. Therefore, in pavements, it is neglected for simplicity (Al-Qadi, et al., 2008)

Mode I
(Opening)

Mode II
(Sliding)

Mode III
(Tearing)
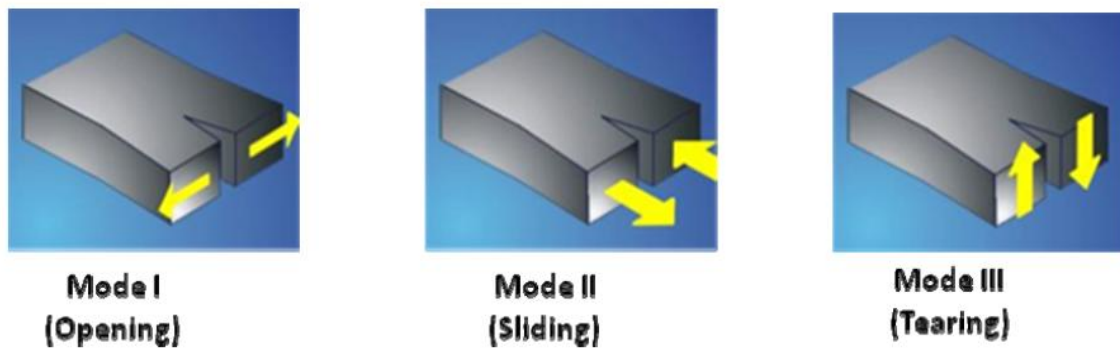
Figure 2-1 Modes of cracking (Al-Qadi, et al., 2008)

Sawcut joints are placed in Portland cement concrete PCC to control and minimize the random cracking created by environmental forces and concrete shrinkage which build

up tensile stresses in concrete; the joint creates a weakened section causing the cracks to form at these specific locations (Suprenant , 1995). These forces are most acute during the first 72 hours after placing the concrete as is still gaining strength (CPTP, 2007). Therefore, when the tensile stresses exceed the tensile stress of concrete, the crack is induced beneath the joint as shown in (Figure 2-2). This type of joints is called contraction or control joint (Suprenant , 1995), they are transverse joints used to relieve tensile stresses (Huang, 1993).
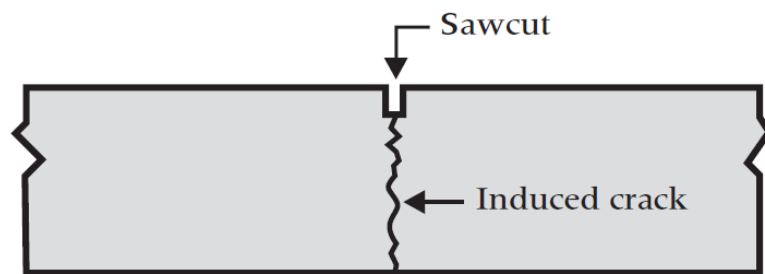
Figure 2-2 Cross section of contraction joint (ISU, 2004)

2.4 Fundamentals of reflective cracking

Reflective cracking is one of the most serious problems associated with the use of thin overlays. This phenomenon is due to the horizontal and vertical movement of the underlying pavement layer caused by external loading (Figure 2-3) and thus resulting in shearing and tearing of the overlay (Cleveland, et al., 2002).

9
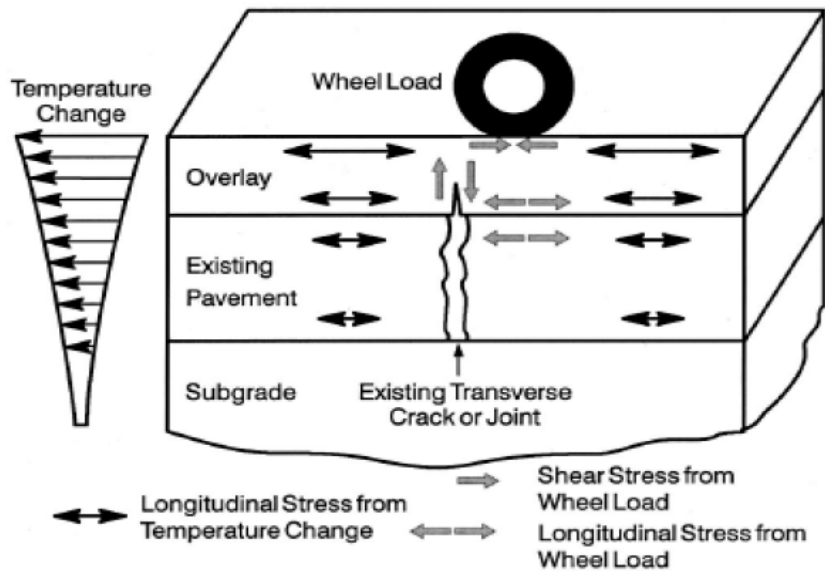
Figure2- 1 Reflective cracking and principal crack driving forces (Kim & Buttlar, 2002)
Reflective cracks are caused by joints or cracks existed in the underlying layers that
propagate through the new overlay (Al-Qadi, et al., 2008).

The major driving forces of the phenomenon of reflective cracking are:

1- The external wheel load: This leads to high stress and strain in the overlay above the
existing crack where the bending stiffness of the rehabilitated pavement section is
reduced due to the discontinuity in the existing pavement creating stress
concentration (Khodaii & Fallah, 2009). When the stress value exceeds the fracture
resistance of the overlay, a crack is initiates and a combination of mode I and II
leads to crack propagation through the overlay (De Bondt, 1998).

2- Daily temperature variations: The movement of the discontinuous underlying
pavement caused by temperature changes results in additional concentrated tensile

stresses in the new pavement above the existing crack or joint; this phenomenon is directly related to the mode I crack opening mechanism (Kim & Buttlar, 2002). Temperatures in pavement change very slowly over the hours of the day; whenever loading or temperature changes, reflective cracks in the old pavement grow. (Lytton, 1989) Suggested that embedding a geotextile layer in the asphalt overlay is one way to retard the growth of reflective cracks.

Three pulses of high of high stress concentrations as pointed out by (Lytton, 1989) occur at the tip of the crack every time a load passes over a crack in the old pavement (figure 2-4). A maximum shear shown at point A in (figure 2-4) is the first stress pulse. It is followed by a second maximum bending stress pulse shown at point B in (figure 2-4). The third stress pulse is a maximum shear stress pulse in the opposite direction of the first shear pulse. The maximum shearing stress pulse is greater at point C than point A, because there is often a void beneath the old surface. Small increase in crack length in the overlay is a result of pavement movement. When the number of loadings increases, the magnitude of movement increases as well as the crack growth rate, and overlay reflection cracks rapidly appear at the pavement surface.
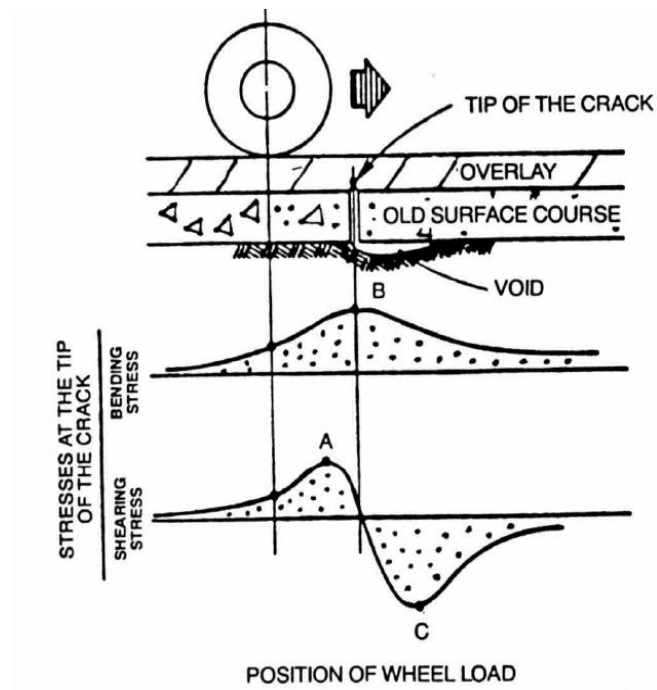
Figure 2-4 - Shear and bending stress induced at a crack caused by a moving wheel load (Lytton, 1989)

2.4.1 Methods of reducing reflective cracking

The methods described in the literature were in general attempting to increase the tensile strength of the overlay or to decrease/redistribute the stress at the bottom of overlay (Aldea & Darling, 2004). Huang has categorized four possible combinations depending on the type of overlay and existing pavement (Huang, 1993):

1- Hot mix asphalt(HMA) overlays on asphalt pavements

2- HMA overlays on Portland cement concrete (PCC) pavements

3- PCC overlays on asphalt pavements

4- PCC overlays on PCC pavements

However, as mentioned earlier, the major challenge in designing an overlay is reflective cracking. Several methods were reported by (Barksdale, 1991) (Huang, 1993) (Roberts, et al., 1996) (Cleveland, et al., 2002) in the literature to address the issue of reflective cracking and to minimize it. The following are the methods of reducing reflective cracking in HMA overlays over PCC pavement:

1- Increase the thickness of HMA overlay

2- Crack and seat the existing PCC slab into smaller slabs.

3- Use a crack relief layer with drainage system

4- Saw and seal joints in an HMA overlay

5- Use a stress-absorbing membrane interlayer with an overlay

6- Incorporate a fabric membrane interlayer with an overlay

2.5 Reinforcement

The lack of tensile strength within the pavement materials is compensated by the usage of reinforcement. In any reinforcement application, the reinforcing material should be stiffer than the material to be reinforced (Rigo, 1993). The reinforcement mechanism is now better understood due to the earlier work done by Lytton and Monismith, where major outlines were defined for the requirements from an interlayer system to act as reinforcement (Lytton, 1989) (Monismith & Coetzee, 1980). The reinforcement failure mode was summarized by (Button & Lytton, 1987) as follows: Due to thermal and traffic loading, the cracks start propagating from its origin upward until reaching the reinforcement layer. The crack then will turn laterally and move along the interface until

losing its energy, when the interlayer is stiff enough. (Lytton, 1989) Reported that the

failure in the reinforcement would develop only after the debonding between the lower

layer and the interlayer (Lytton, 1989).It can be concluded, from this mechanism, that the

reinforcement would be successful only if the interlayer is sufficiently stiffer than the

material to be reinforced. The stiffness of an interface is equal to the material elastic

modulus times its thickness (Barksdale, 1991). Based on the mentioned above, a

reinforcement interface may contribute to the structural capacity of the pavement.

2.5.1 Steel-reinforced concrete

The conventional reinforcing method that has been used in reinforced Portland

cement concrete pavements is reinforcing with steel bars. Considering the fact that steel

reinforcement provide the necessary strength required to endure stresses applied by moving

loads. Steel-reinforced concrete, with proper design and execution, is a functional and

durable construction material. However, several constraints often limit the use of that

method. Some of the limitations include physical constraints of placing the reinforcing steel

bars in thin elements, such as thin overlays, in addition to the extensive time of construction

and the concerns of corrosion (Nawy, 2000). In the case of bonded concrete overlay, where

the section is 2 in thick, the use of steel reinforcement is not possible due to insufficient

concrete cover. As a result of this inadequacy, many risks will arise such as steel corrosion

and car wheels damaged due to exposed steel bars. Therefore, the need arises for

alternatives to replace the reinforcing steel bars; An Experimental study was conducted by

(EL Meski & Chehab, 2014) on the flexural behavior of concrete beams under four-point

bending and reinforced with different types of geogrids and they concluded that all types of

geogrid reinforcement provide a ductile post-cracking behavior, high fracture energy, high

flexural strength and large deflection.

2.6 Geosynthetics

Geosynthetics have long been used to enhance the performance of engineering

structures, in particular for the geotechnical applications (Palmeira, et al., 2008)as they are

used as reinforcing and stabilizing agents in various heavy civil and infrastructure works

(Maxwell, et al., 2005). They are also used in pavement applications (Dhule, et al., 2011).

Geogrids are particular type of geosynthetics, they are usually stiff materials formed

into a grid like structure with large apertures (Koerner, 1994). The main role of geogrids is

to provide a reinforcement function (Zornberg, et al., 2008).Geogrids provide an

interlocking mechanism with the surrounding material due to the uniformly distributed

apertures between the longitudinal and transverse ribs. As a result of the increased

interlock, when incorporated in geotechnical applications, the bearing capacity of soils is

increased (Rajeshkumar, et al., 2010).

In pavements, geogrids restrain the lateral movement of the aggregate layers under

traffic loading by confining those layers (Kwon & Tutumluer, 2009). Geogrids have also

been used as reinforcements in asphalt pavement layers (Al-Qadi, et al., 2008) resulting in

reduction in the rutting and fatigue cracking of pavement, therefore extension in their useful

service life (Dhule, et al., 2011).The use of geogrids as interlayers has become widely used

to mitigate reflective cracking in asphalt overlays of jointed plain concrete pavements (Khodaii & Fallah, 2009).

Little investigation has been done on the use of geogrid as main reinforcement in thin Portland cement concrete elements, such as overlays in pavements, where using steel reinforcement is not possible (Tang, et al., 2008). Moreover, (EL Meski & Chehab, 2014) have conducted an experimental study on the flexural behavior of geogrid reinforced concrete beams and they concluded that the use of geogrid as reinforcement in concrete provide a ductile postcracking behavior, high flexural strength and fracture energy, and large deflection.

2.6.1 Physical and mechanical properties of geogrid

The physical and mechanical properties of geogrids have an important role in the reinforcing effectiveness for concrete; it was noted by (Tang, et al., 2008) that the difference in the performance for geogrids for the same concrete mixture is due to difference in the physical and mechanical properties of geogrids (Tang, et al., 2008).

Type of geogrid, aperture size, thickness, weight, and width are the physical properties of geogrid. Those properties are crucial in the selection process since economic considerations and convenience of handling should be taken into consideration (Abdelhalim, 1983) (Koerner, 1994).

To use as reinforcement material, geogrid must provide high tensile strength to the pavement system. To measure the tensile strength of geogrids, they should be placed within

a set a clamps and stretched from the ribs until failure occurs (Koerner, 1994). During this process, a stress-strain relationship is graphed from both measurement of load and deformation. Thus valuable information is obtained such as: maximum tensile stress, maximum elongation, toughness and elastic modulus.

As for the geogrid stiffness, (Tang, et al., 2008) concluded that higher total energy absorption capacity and additional post-cracking ductility are witnessed in concrete beam reinforced by stiff geogrid. (Abdelhalim, 1983) Also concluded that the geogrid should be stiff enough to withstand vertical stresses and flexible enough to distribute the stresses uniformly and reduce the intensity to underlying layers.

CHAPTER 3

MODE I CRACKING (DIRECT TENSION TEST)

The direct tension test of concrete has been given little attention by researchers, due to the difficulties in applying direct tension loading to concrete specimens (Kim & Taha, 2014). They tend to use indirect tension methods to study the tensile properties of concrete due to their simplicity, such as split cylinder test and beam flexure test. In these test, the tensile stresses are being applied indirectly to the specimen. In the split cylinder test, a concrete cylinder is placed horizontally in a compression machine between two plates loaded until failure by splitting. In the flexure test, like three points or four points bending, a concrete beam is subjected to bending until flexural failure. Even though the criteria of load carrying is not relied upon the tensile strength of concrete, it is essential to study the behavior of concrete in tension due the fact that many structural failures are associated with cracking which reduces the integrity of the concrete structure (Zheng, et al., 2001). The tensile properties of concrete are important in the study of mitigating reflective cracking, since the concrete pavements are subjected to tensile stresses, such as those due to temperature differentials and drying shrinkage (Swaddiwudhiponga, et al., 2003). By using the direct tension test, this study investigates the effect of inclusion of geogrids in thin concrete member under mode I cracking which is the opening mode due to thermal loading.

3.1   Proposed test method

The direct tension test is usually conducted by applying fixity to one end of a specimen and loading to the other end. The common ways of performing the direct tension test presented in the literature were by using friction grips to clamp the ends of the concrete (Saito & Imai, 1983), gluing the end of the specimen with epoxy, or by casting steel studs into the concrete specimen (Xie & Liu, 1989). However, these methods suffer from a major problem which is inducing secondary stresses at the ends causing uneven stress distribution and localized failure (Zheng, et al., 2001). To avoid the end effects the specimen ends should be enlarged. In this study, an FEM model of the direct tension test was developed using "ADINA" (ADINA, 2012) to come up with the optimal specimen configuration, a specimen that does not suffer from stress concentration at boundaries. Based on that, it was decided to use a notched dog bone shape with 14 mm steel threaded rods into the concrete specimen (figure 3-1). The height of the samples is 40cm and the largest cross section is (7x10cm) and the smallest section is (2.5x10cm) (figure 3-2).
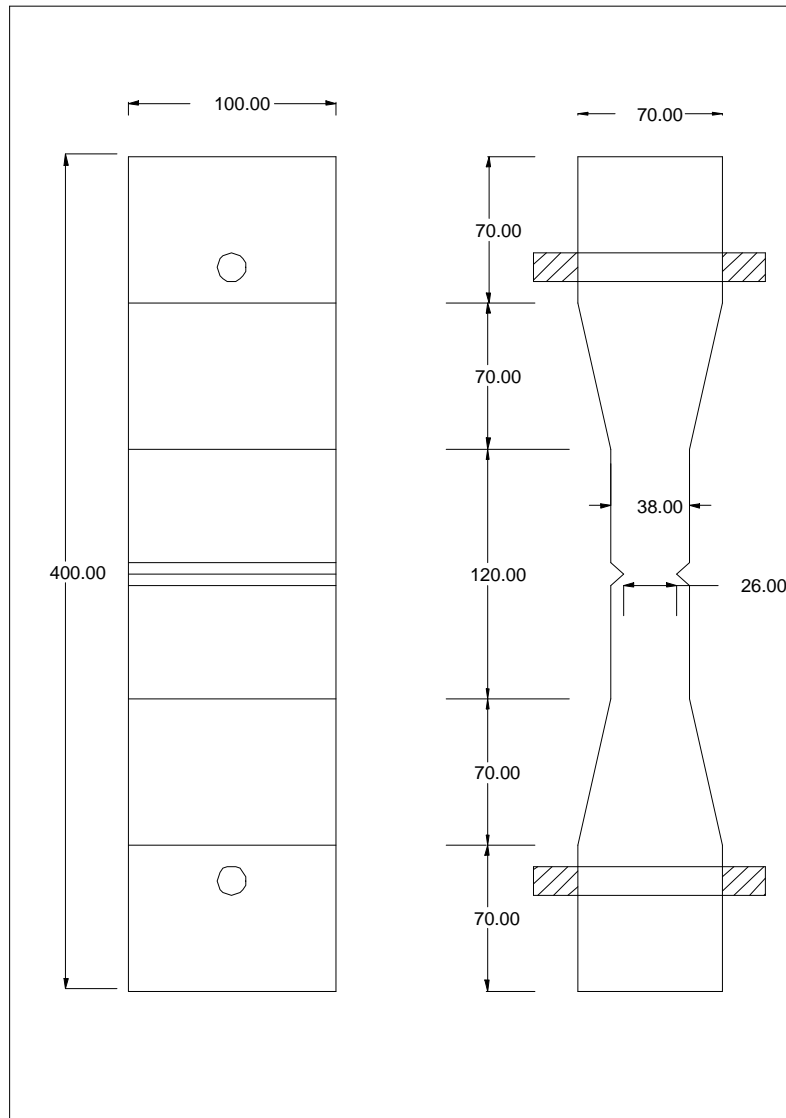
Figure 3-1 Adopted sample

Figure 3-2 Schematic of the adopted sample

The FEM trials results show that the adopted configuration has the ability to distribute the tensile stress almost uniformly as shown in (figure 3-3), where the tensile stress is within ±1.75% of the average stress.
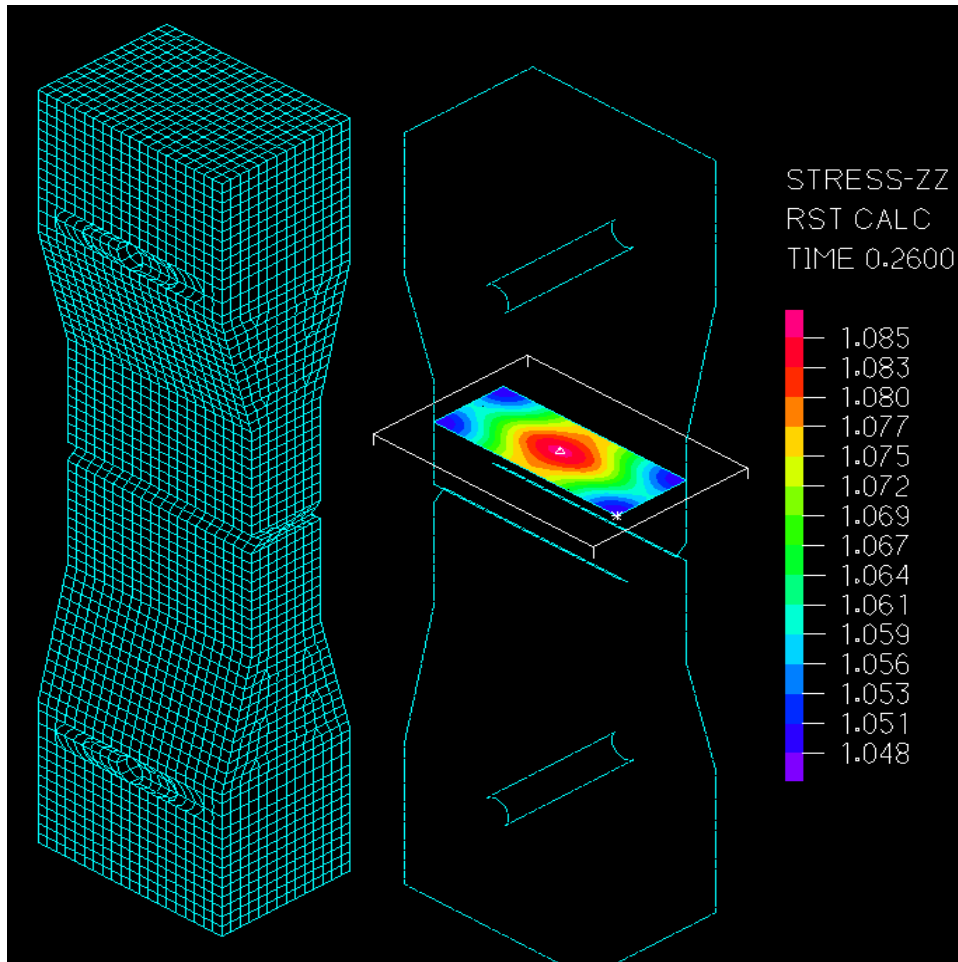
Figure 3-3 Tensile stress distribution at the reduced section where the strain experimentally is measured

The threaded rods are to be used for applying the load and fixity on the specimens. An assembly of steel plates is used to fix the specimen with the machine from the actuator and the base sides. (Figure 3-4) is showing the adopted concrete specimen and the final testing setup.

The direct tension test is conducted using a Universal Testing Machine of a capacity of 25 KN with computerized test control and data acquisition system "UTM-25". The load is applied gradually until failure in displacement control at a constant rate of 0.0133

mm/sec. The displacement at the middle of the specimen was measured by vertical spring

loaded Linear Variable Differential Transducers (LVDT) which were fixed on the sides of

the specimen using epoxy. The test was performed at room temperature

Figure 3-4 Testing setup

3.2   Testing program and materials

Six specimens were prepared for testing. One of normal strength Portland Cement

Concrete mixture was used in the study. Among the prepared specimens, three of them

were plain concrete with no reinforcement to serve as control and the others were

reinforced with uniaxial geogrid. Uniaxial geogrids exhibit high tensile strength in its

unidirectional ribs (EL Meski & Chehab, 2014). The geogrid layer was placed at the middle longitudinal section.

The stress-strain curve of uniaxial geogrid was obtained from the direct tension test applied on 4 geogrid samples (figure 3-5), S stands for geogrid sample and the second number is the replicate number. The uniaxial tension test setup of the geogrid sample is shown in (figure 3-6). Friction grips were used to hold the geogrid at the junction location. The load was applied gradually until failure. The modulus of elasticity of geogrid is calculated from the 4 samples (figure3-7) and the average value (E=2290 MPa) was used in the analysis. This modulus is calculated in the linear elastic region at low strains.
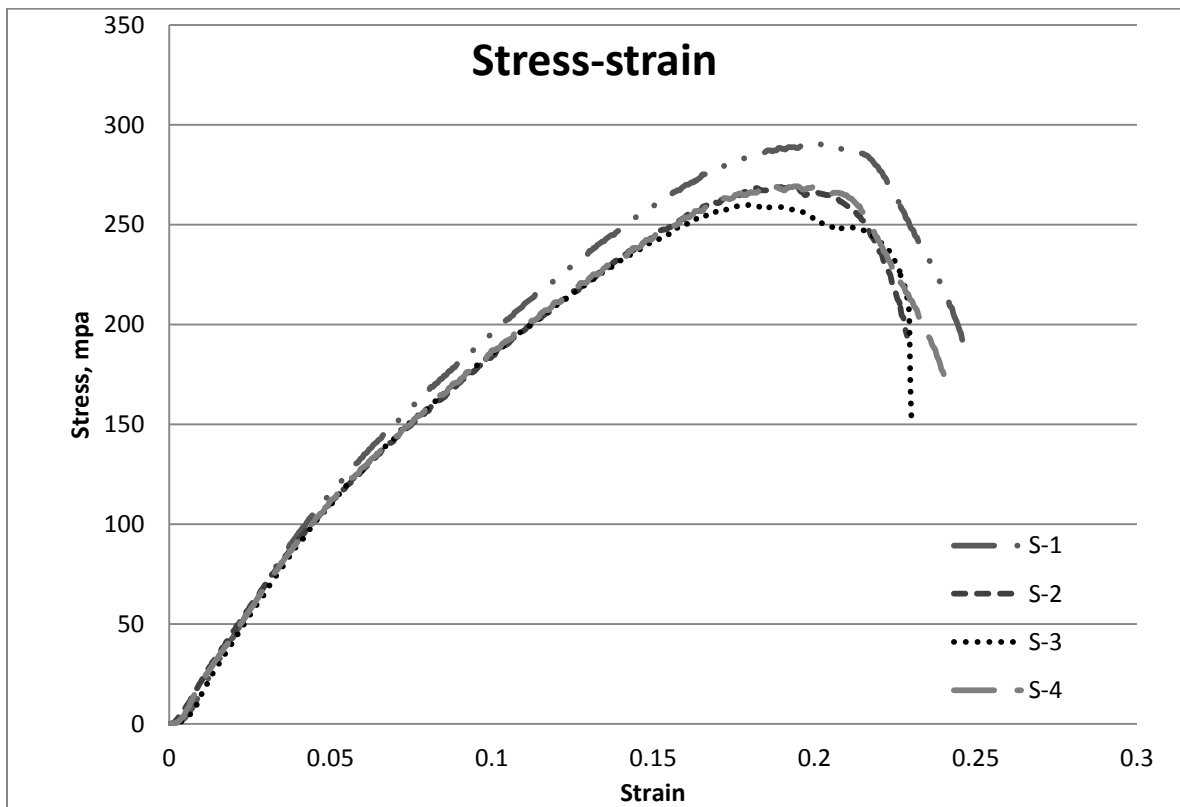

Figure 3-5 Stress-strain curve of the uniaxial geogrid used in testing
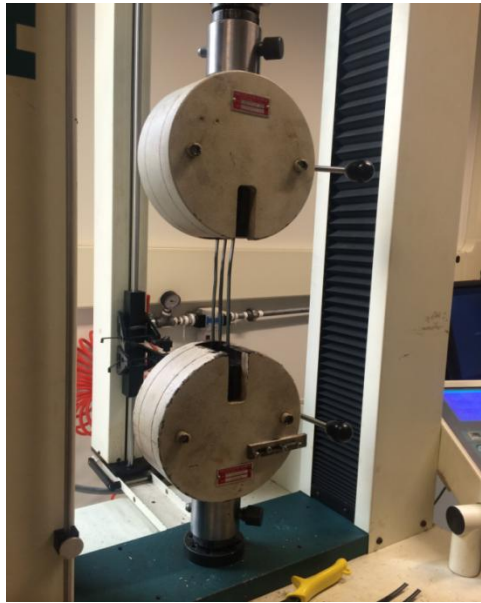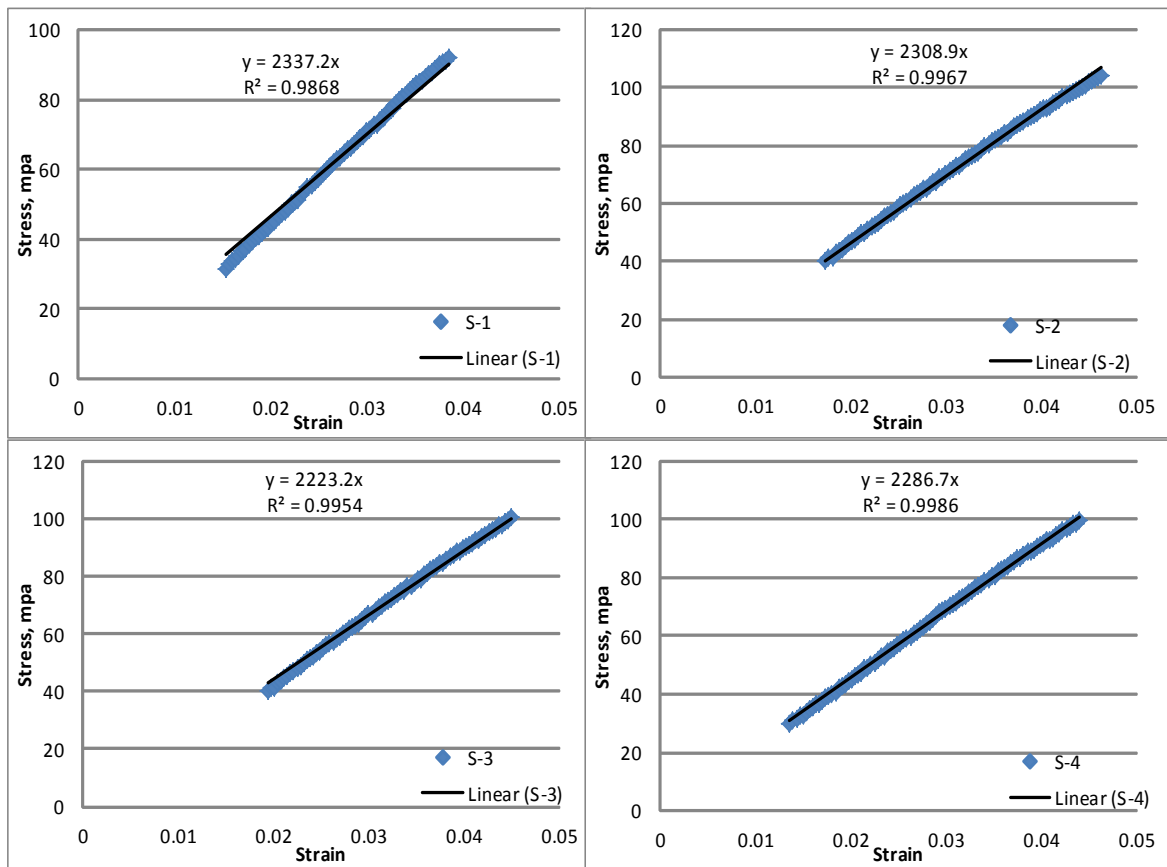
Figure 3-6 Geogrid sample tested in tension

Figure 3-7 Modulus of elasticity calculation

Type I Portland cement, natural sand and fine aggregates were used for the concrete mix. The used sand was dry and the aggregates were clean from the dust and fine particles. The concrete mix was designed to produce a cylindrical concrete compressive strength of 29 Mpa at 28 days. The specimens were placed in a curing room for 12 days with continuous wetting cycles at a temperature of $23\pm5^{o}C$ and relative humidity greater than 95%. The maximum aggregate size of the PCC mixture was smaller than the aperture dimensions of the uniaxial geogrid. Such condition provides adequate interlock and prevents potential blocking by allowing all aggregates to pass through the aperture.

Wooden molds were fabricated for the specimens. To create a triangular notch, a strip of Plexiglas was glued to the sides of the mold at mid length; the cross section of the notch is 11.2 mm wide and 5.8 mm deep. The mixing of concrete for the 6 specimens was done in one batch using a concrete mixer with 0.05 m^3 capacity. Three cylinders were casted from the batch.

For the specimen designation (figure 3-8), the first letter P stands for plain concrete (control samples) and G stands for geogrid reinforced samples. The second number is the replicate number.

Figure 3-8 Casted concrete samples

3.3   Finite element analysis of the test setup

For the analytical part of this study, nonlinear finite element models were built

using the Automatic Dynamic Incremental Nonlinear Analysis "ADINA" (ADINA, 2012).

The specimens were discretized in three dimensions. Two 3 dimensional models were

created, the first one is the plain concrete model and the second is the geogrid reinforced

model (figures 3-9 & 3-10). An incremental solution process was used using the full

Newton method. The magnitude of the displacement load was selected in a way to cause failure of the specimen.

The FEM mesh consists of three dimensional solid elements with 8 nodes each. The constitutive material model for concrete is the concrete model found in ADINA's material library. It is a nonlinear, multi-axial constitutive model which has the characteristic of failing in tension at a maximum, relatively small, tensile stress and a crushing failure due to high compression (ADINA, 2012). As for the geogrid material, the modulus of elasticity obtained from testing was defined as isotropic linear elastic material in ADINA. The input parameters of the models are represented in table (3-1) & (3-2)

Input Parameter	Value
Tangent modulus at zero strain	26926 mpa
Poisson's ratio	0.19
Uniaxial cut-off tensile stress	1.55 mpa
Uniaxial maximum compressive stress	29 mpa
Uniaxial compressive strain	0.002
Uniaxial ultimate compressive stress	26 mpa
Uniaxial ultimate compressive strain	0.003

Table 3-1 Concrete material input parameters

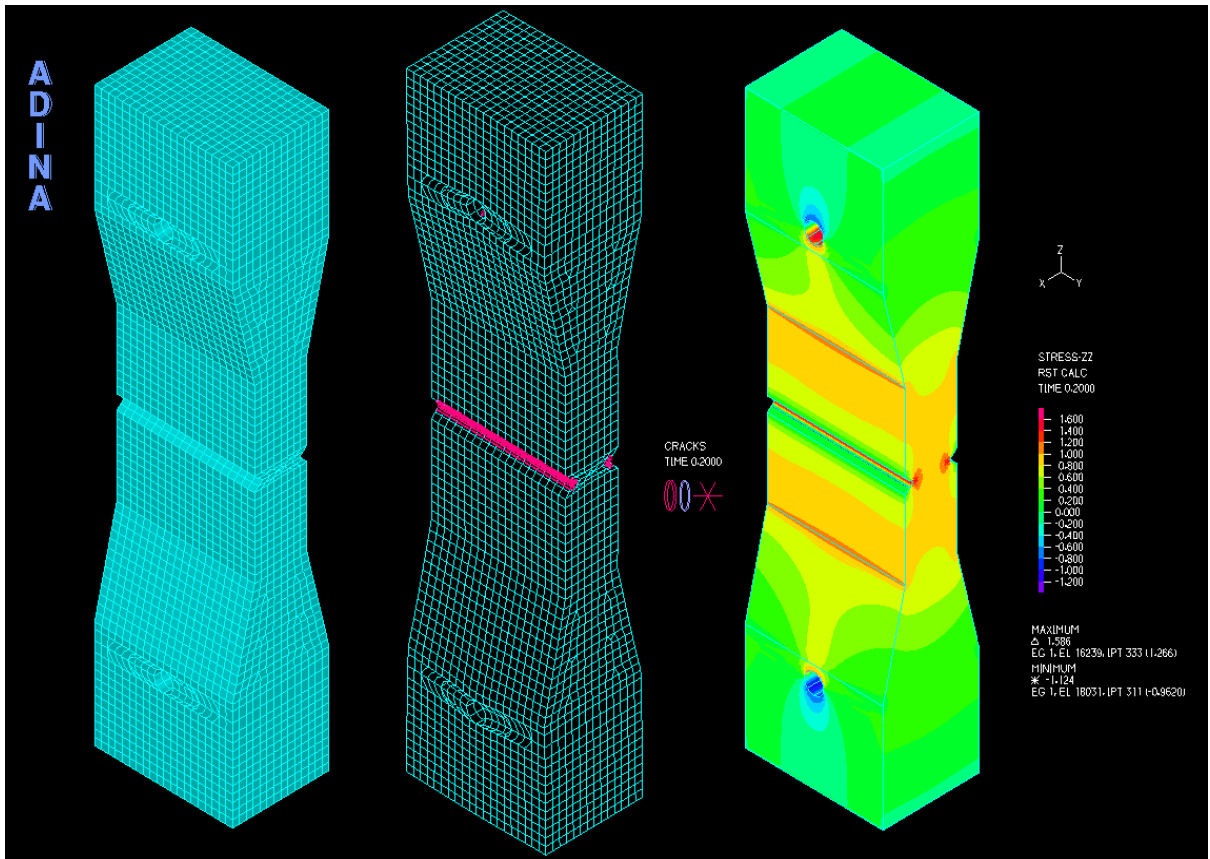| Input Parameter	Value
Modulus of elasticity	2290
Poisson's ratio	0.3

Table 3-2 Elastic material input parameters

Figure 3-9 Plain concrete model, cracks location and tensile stress distribution
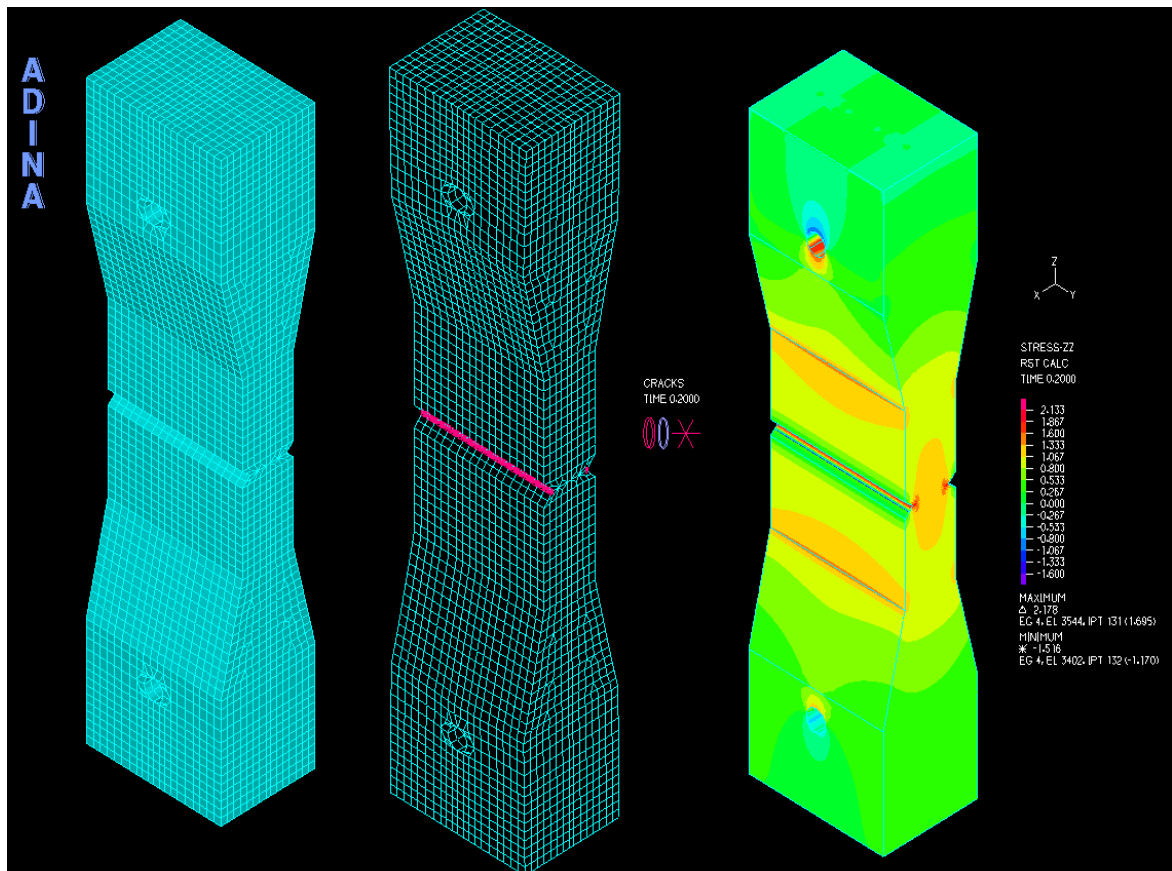
Figure 3-10 Geogrid reinforced concrete model, cracks location and tensile stress distribution

3.4   Results and analysis

During the test, loading was applied gradually. Once the stress in the concrete

reached its strength value, a crack initiates at the location of higher stress which is the

notch. (Figure 3-11) shows a typical plain concrete failed specimen, the ending of the test

was when the concrete completely failed and the specimen split in half. This behavior is

attributed to the brittle failure of concrete with the lack of any reinforcement. Whereas for

reinforced samples, the concrete and the geogrids were absorbing tensile stress; after

cracking of concrete the load is redistributed in a way that it is completely absorbed by the

geogrids as clearly shown in (figure 3-12) which is a typical geogrid reinforced concrete failed specimen.

It is worthy to mention that during testing and analysis it was noticed that the LVDTs were recording almost similarly. This is a good indication and it means that the specimen is not tilting and it is perfectly aligned and as a result the load will be distributed uniformly over the area.

Figure 3-11 Plain concrete mode of failure

Figure 3-12 Geogrid reinforced concrete mode of failure

3.4.1   Effect of reinforcement on load-displacement response

Figure 3-13 presents the load-deflection curves for both plain and geogrid-reinforced concrete in direct tension test. Just after initial cracking of concrete, both exhibit sudden drop in load. As for the failure mode, the plain concrete specimens follow a brittle failure due to the lack of any reinforcement. However, the geogrid-reinforced samples exhibit cracking delay and an increase in strength after cracking. It is also shown from figure 3-13 that the geogrid-reinforced samples undergo significant deformation after initial cracking due to the geogrid ductility. But, the deformation in the plain concrete samples after initial cracking and before total failure is relatively small. This extensive deformation shows that the inclusion of geogrid provides post cracking ductility.

3.4.2   *Effect of reinforcement on maximum load capacity and fracture energy*

It is noticeable from (figure 3-13a, b) that the maximum load capacity of the geogrid-reinforced sample is greater than the plain concrete. The cracking of concrete happens just after reaching the maximum load capacity of the section. Therefore, the initial cracking is delayed as a result of the increase in strength.

The fracture energy is defined by the area under the load-displacement curve. The more required energy for a crack to open the more resilient the section is. As shown in (figure 3-13b) the inclusion of the geogrid leads to an increase in the fracture energy.
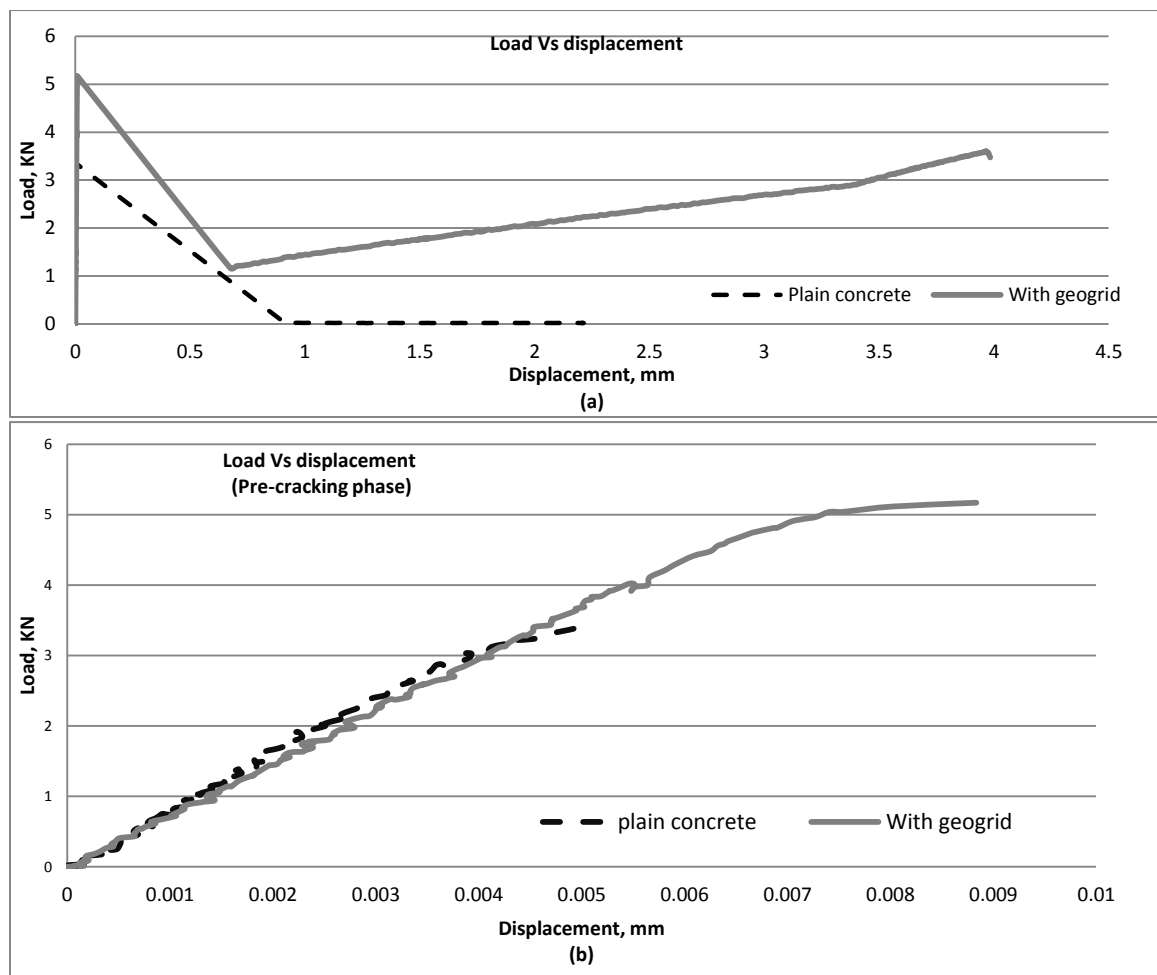
Figure.3-13 a) Load Vs displacement curves, b) load vs displacement (pre-cracking phase)

3.4.3 *FE model calibration*

The results from the experimental work were used to calibrate the FE models for later use and investigation as shown in (figure 3-14). First the concrete model was calibrated to get the properties of concrete. After that these properties were used in the calibration of the geogrid concrete model.

Plain model calibration — Load, KN vs Displacement, mm

Legend: Plain concrete (experimental), ADINA plain

(a)

Geogrid model calibration — Load, KN vs Displacement, mm
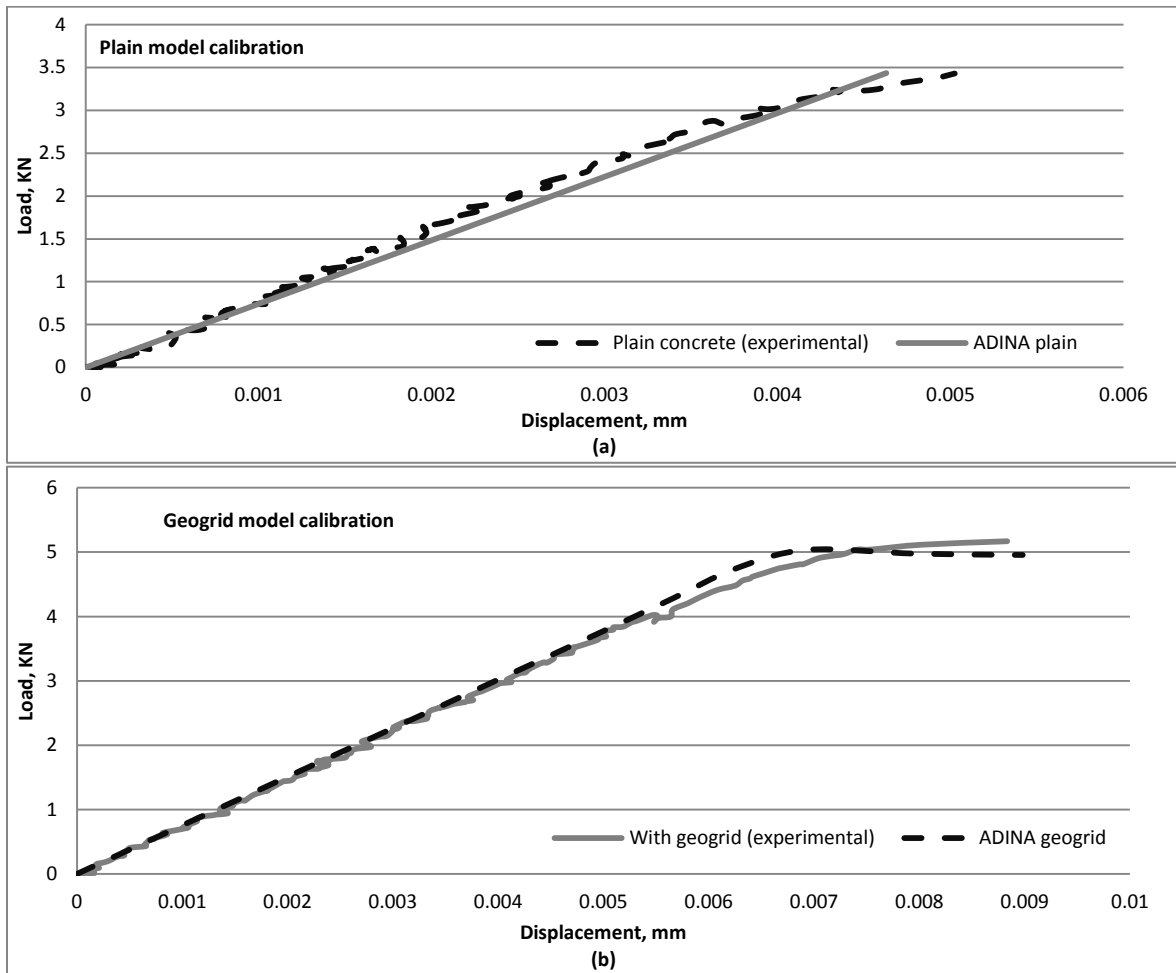
Legend: With geogrid (experimental), ADINA geogrid

(b)

Figure 3-14 FE model calibration for a) plain concrete and b) geogrid reinforced concrete

Two FEM models were created to see the effect of temperature change in concrete overlays. The first model is plain concrete and the second is reinforced with geogrids (figures 3-15 & 3-16)
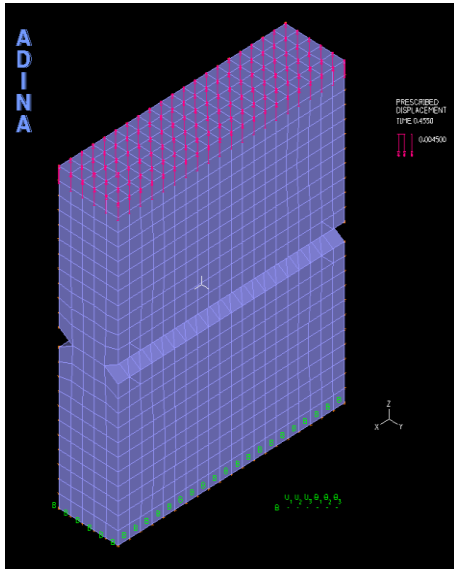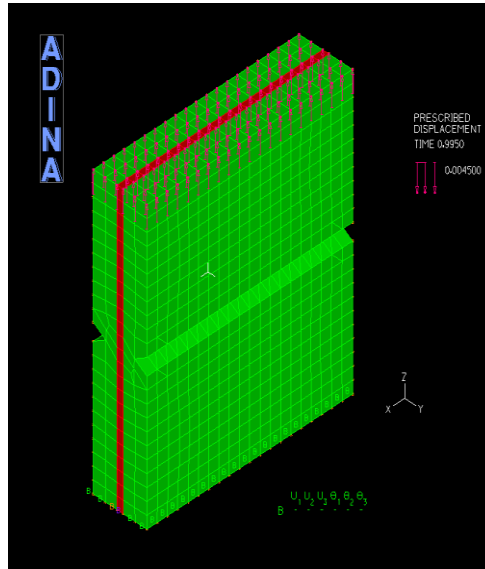
Figure3-15 Plain concrete model   Figure3-16 Geogrid concrete model

The bottom face of the sample was fixed and cyclic triangular loading was applied on the top of the specimen. The magnitude of the displacement load was 0.0045 mm. This amount is due to a rise or fall of 3.75 degrees Celsius for this specimen.

It was noticed that the geogrid has increased the life of the overlay by 55% where the plain concrete specimen failed at the 8th time step and the geogrid sample failed at the 18th time step. Figures 3-17 and 3-18 show the stress and strain values with respect to time. Plain concrete model witnessed a drop in the stress after initial cracking and the decrease continue until complete failure; this can be seen also from the strain curve which starts to increase dramatically after initial cracking. This is not shown in the geogrid reinforced model where stress and strain are maintained after initial cracking at almost constant values until complete failure.
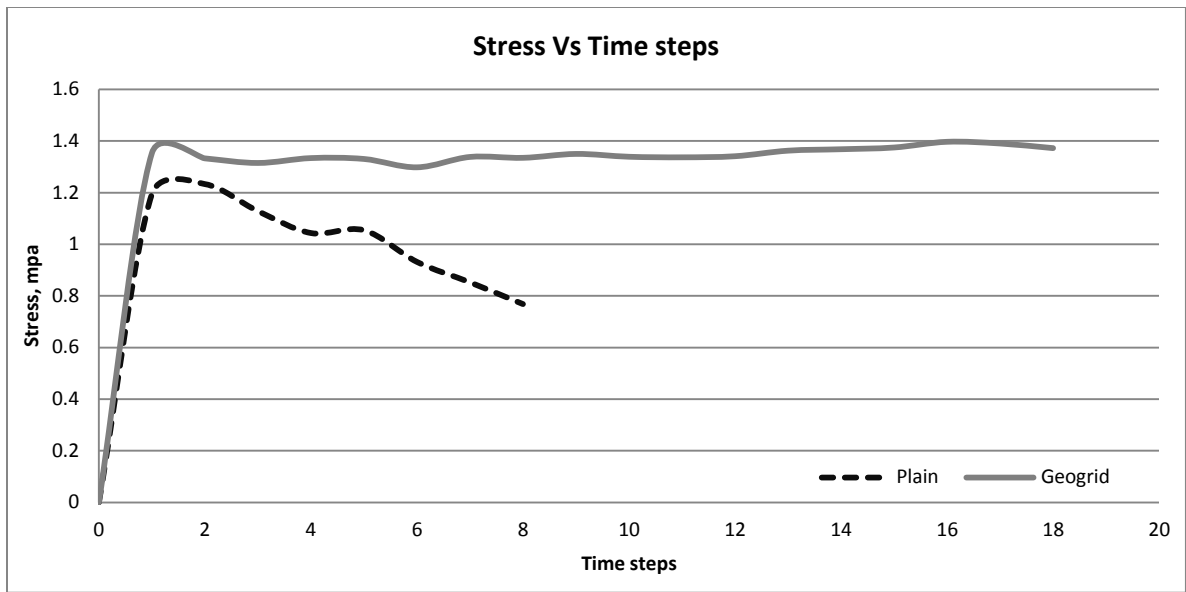
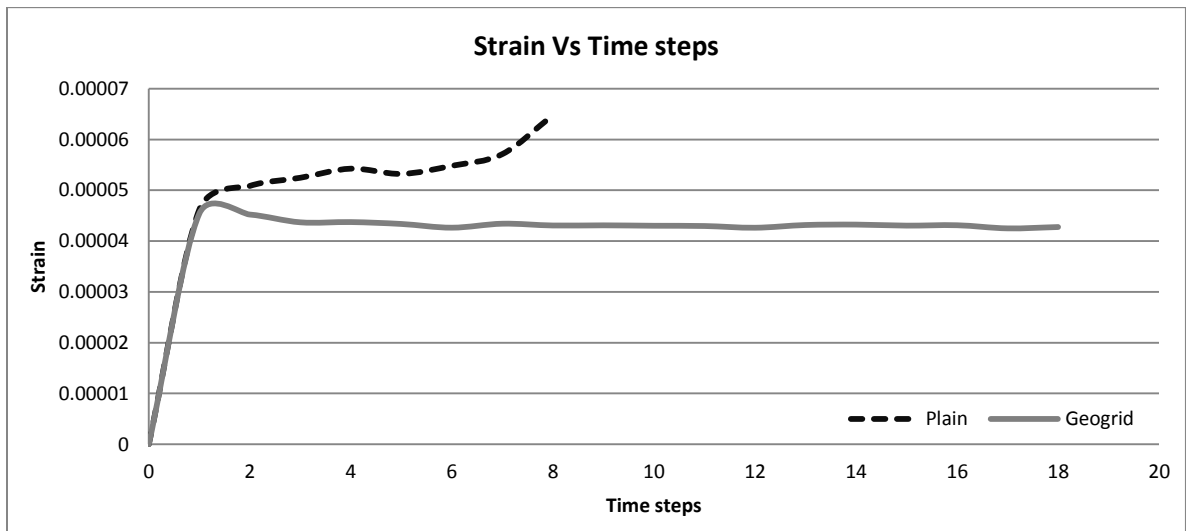Figure 3-17 Stress Vs time steps for plain and reinforced concrete models

Figure 3-18 Strain Vs time steps for plain and reinforced concrete models

CHAPTER 4

MODE I CRACKING (FLEXURE TEST)

4.1 Test setup

The traffic and thermal loads are considered to be different, even though they both produce tensile stresses at the bottom of the overlay (Gonzalez-Torre, et al., 2015). In the current study, a new test setup was used to evaluate the effects of using geogrids to reinforce overlays under bending mode (mode I) (figure 4-1). It consists of the following components: (a) a notched concrete overlay 380mm x 150mm x50 mm, which may be plain concrete or reinforced with geogrids at one third of the depth and (b) a 30 mm neoprene rubber base with an elastic modulus of 100000 KN/m^2 to serve as resilient subgrade.

The loading was applied on the top center of the concrete slab through a circular loading plate (138 mm diameter). A soft rubber is placed between the steel plate and the concrete to allow the perfect support on the specimen. Two types of loading were adopted in this study monotonic and cyclic loading. For the monotonic, the load was applied at a constant rate until failure. The simulated moving loading was applied to the specimens using a hydraulic dynamic loading frame. The loading wave shape was haversine. Loading was applied with a frequency of 10 Hz to simulate high speed traffic. To model a truck wheel load, 100 psi pressure (690 KN/m^2) was applied at the top center of the plate. A 50 KN/m^2 minimum pressure was used to keep the loading plate in place during dynamic loading. The test is conducted using a Universal Testing Machine of a capacity of 25 KN

with computerized test control and data acquisition system "UTM-25". The test was

performed at room temperature.
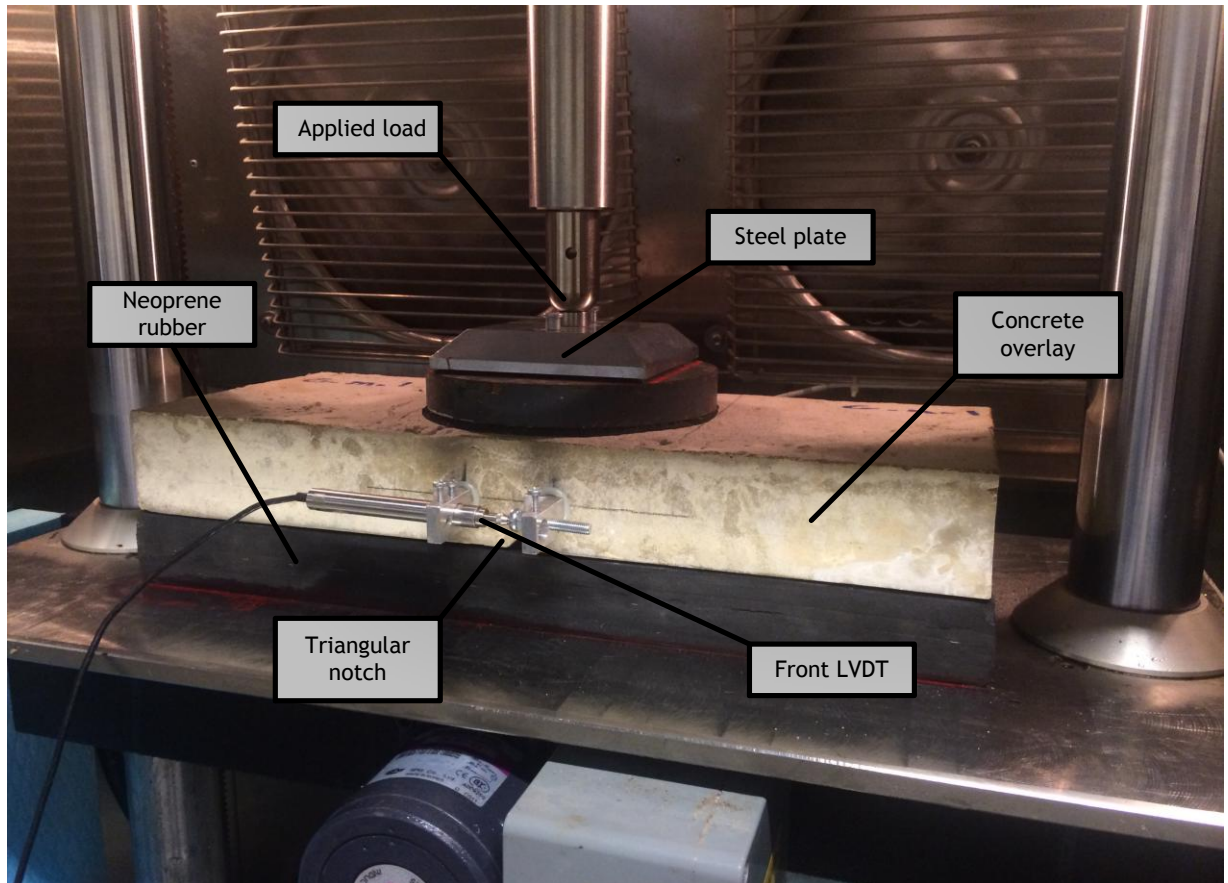
Figure 4-1 Flexure test configuration setup

4.2 Testing program, materials and specimen preparation

A total of 12 notched slab specimens were casted for the test. 6 of them were tested

under monotonic loading and the remaining under cyclic loading. Among the 6 specimens,

3 of them were plain concrete to serve as control samples and the other 3 were reinforced

with uniaxial geogrid. All specimens had a 380mm length, 150mm width and 50mm height

with a triangular notch 11.2 mm wide and 5.8 mm deep across the center of the bottom surface of the slab to induce stress concentration for crack initiation and subsequent propagation. The geogrid layer was placed in the tension zone at one third of the depth.

Type I Portland cement, natural sand and fine aggregates were used for the concrete mix. The used sand was dry and the aggregates were clean from the dust and fine particles. The concrete mix was designed to produce a cylindrical concrete compressive strength of 27 Mpa at 28 days. The specimens were placed in a curing room for 12 days with continuous wetting cycles at a temperature of $23\pm5^{o}C$ and relative humidity greater than 95%. The maximum aggregate size of the PCC mixture was smaller than the aperture dimensions of the uniaxial geogrid. Such condition provides adequate interlock and prevents potential blocking by allowing all aggregates to pass through the aperture. The geogrid used in this test is the same type and has the same properties as the one used for direct tension testing.

Wooden molds were fabricated for the slab specimens. To create a triangular notch, a strip of Plexiglas was glued to the bottom of the mold at mid length; the cross section of the notch is 11.2 mm wide and 5.8 mm deep. The mixing of concrete for the 12 specimens was done in two batches using a concrete mixer with 0.05 m^3 capacity. The specimens were casted in a way to minimize the batch to batch variability on testing results and two cylinders were casted from each batch. The testing later showed that the batch to batch variability was insignificant.

For the specimen designation (table 4-1), the first letter P stands for plain concrete (control samples) and G stands for geogrid reinforced samples. The second acronym, m stands for monotonic loading and c stands for cyclic loading. The third number is the replicate number. As for the concrete cylinders, the first letter B stands for batch, the second number is the batch number and the third number is the replicate number.

Sample	Batch	Cylinder	f'c at 28 days , mpa	Average f'c, mpa	
P-m-1	1				
G-m-2	1	B-1-1	28.63		
P-m-3	1			27.6	
P-c-1	1				
G-c-1	1	B-1-2	26.6		
G-c-3	1				27.1
G-m-1	2				
P-m-2	2	B-2-1	29.26		
G-m-3	2			26.7	
P-c-2	2				
G-c-2	2	B-2-2	24.16		
P-c-3	2				

Table 4-1 Concrete cylinders strength testing at 28 days

For casting the geogrid reinforced samples, a 1.67 cm (one third the depth) concrete layer was first poured and compacted in the mold with a steel rod. To ensure precision, a line was marked on the sides of the molds at one third of the depth using corrector pen. Then, the geogrid layer was carefully installed in the mold. Another layer of concrete was then poured above the geogrid. The intermixing between the concrete layers above and below the geogrid was ensured and no separation or surface voids were observed after de-molding the samples.

During the test, two Linear Variable Differential Transducers (LVDTs) were registering the crack opening. They were installed on both sides of the specimen at a distance of 20 mm from the bottom of the sample. The readings from the two LVDTs were averaged and used in the results.

4.3 Finite element analysis of the test setup

The geometry of the specimen was defined using the ADINA modeler (ADINA-M). The geogrid was modeled using membrane elements that have the same thickness as the geogrid used in testing. The geogrid was modeled as isotropic linear elastic material. The strength of the membrane would be much stiffer than the real geogrid if the actual modulus of elasticity was used. This is because the cross section area of the membrane is much larger than that of geogrid. Thus, the effective modulus should be calculated to compensate the large cross section of membrane by dividing the cross section of the ribs over the cross section of the used membrane (Kuo & Hsu, 2003).

Many researchers have investigated the use of geosynthetics in asphalt pavements and several finite element models have been carried out. A summary of the geosynthetic constitutive model/ element type is presented in (table 4-2)

Author	Geosynthetic constitutive model	Geosynthetic element type
(Barksdale, et al., 1989)	Isotropic linear elastic	Membrane
(Burd & Houlsby, 1986)	Isotropic linear elastic	Membrane
(Burd & Brocklehurst,	Isotropic linear elastic	Membrane

1990)		
(Burd & Brocklehurst, 1992)	Isotropic linear elastic	Membrane
(Dondi, 1994)	Isotropic linear elastic	Membrane
(Miura , et al., 1990)	Isotropic linear elastic	Truss
(Wathugala, et al., 1996)	Isotropic elastoplastic von Mises	Solid continuum

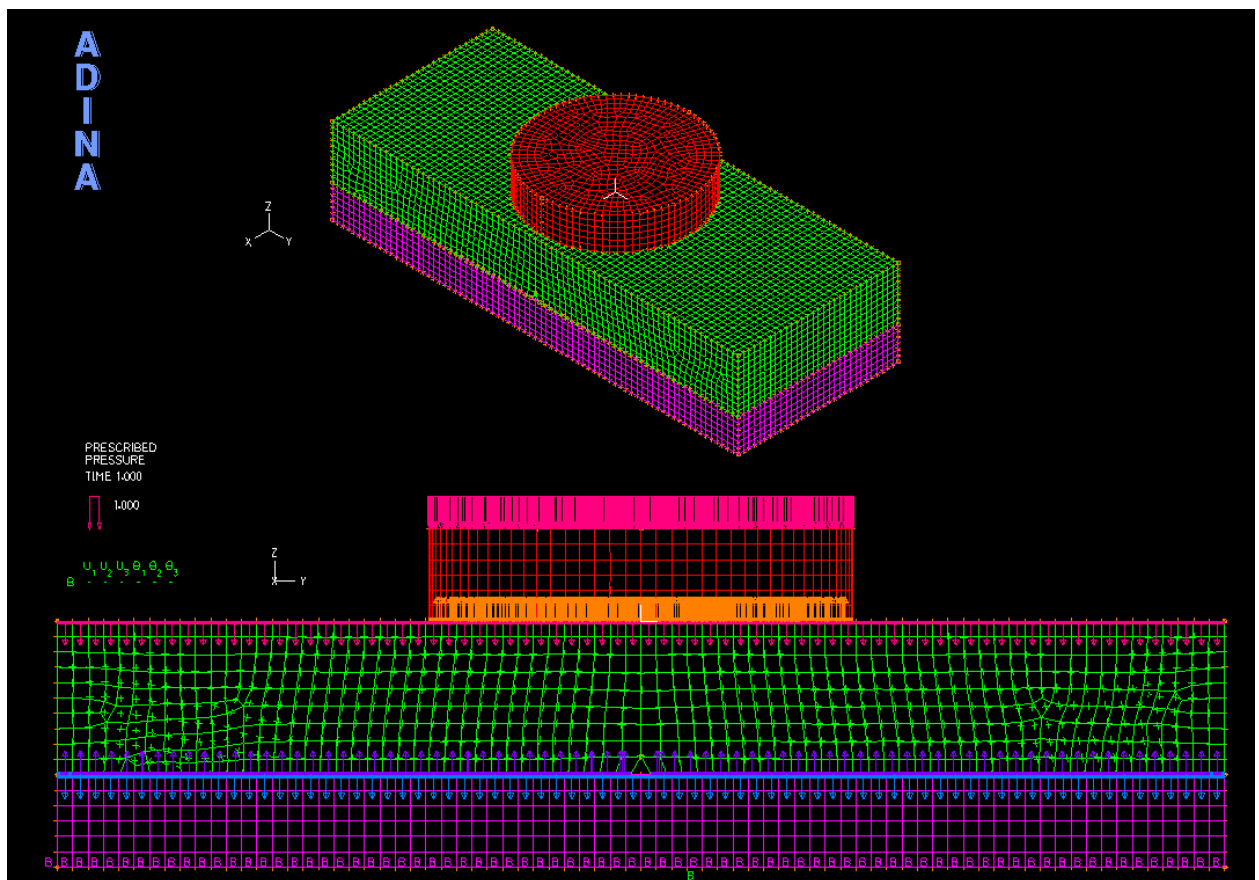Table 4-2 Summary of constitutive model/element type of geosynthetic
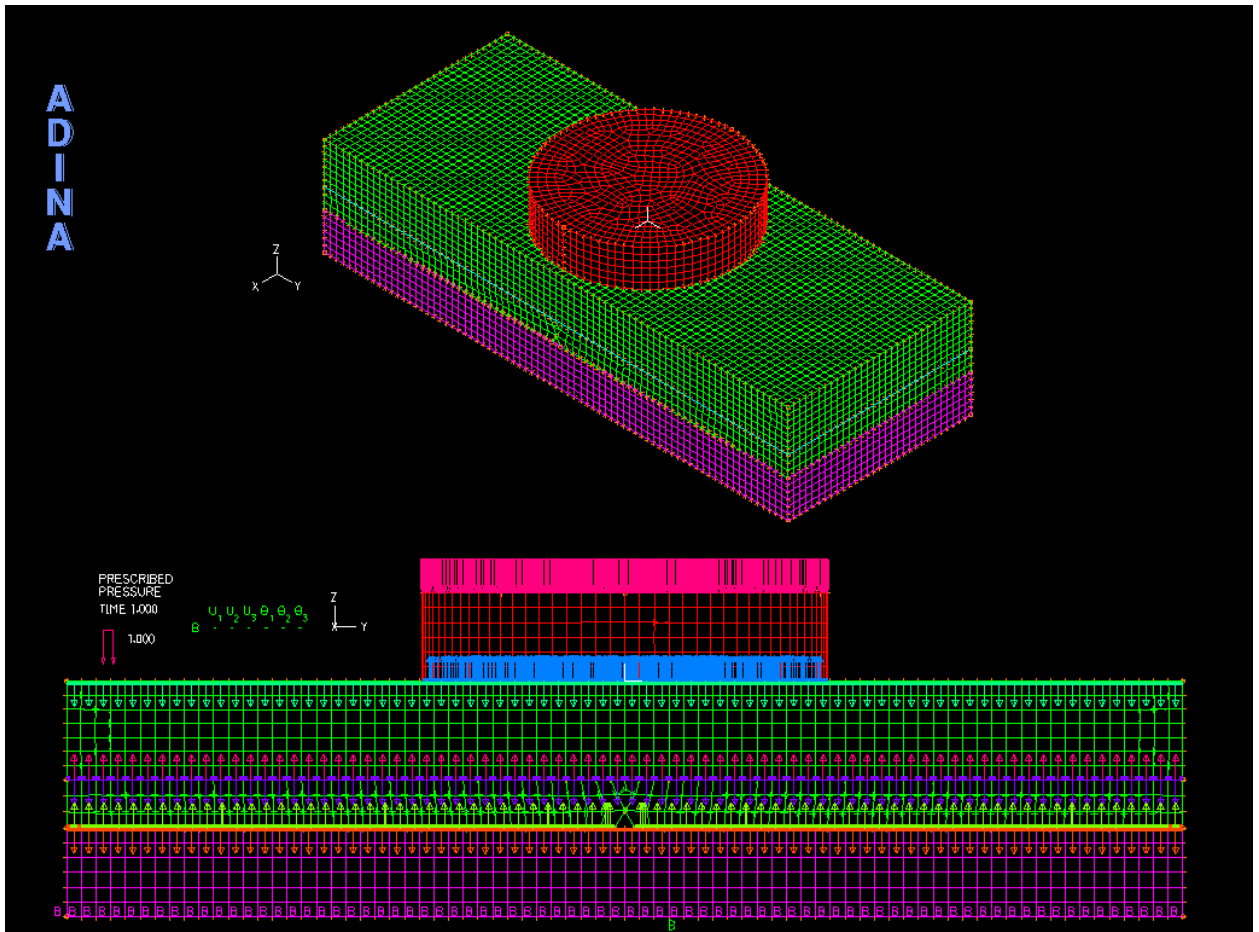

Figure 4-2 Plain concrete model

Figure 4-3 Geogrid reinforced concrete model

4.4 Results and analysis

For monotonic and cyclic loading, the test was conducted until the vertical crack propagated the full depth of the overlay and reached the top of the specimen. When this was not applicable, the test was terminated due to the machine capacity restriction.

(Figure 4-4) shows the evolution of crack starting by initiation from the tip of the notch, widening and further propagation. The screen shots were taken from a recorded video

43

which was played in slow motion. It is worthy to mention that the starting point of the crack in all the specimens was the notch, and none of them occurred away from the notch.
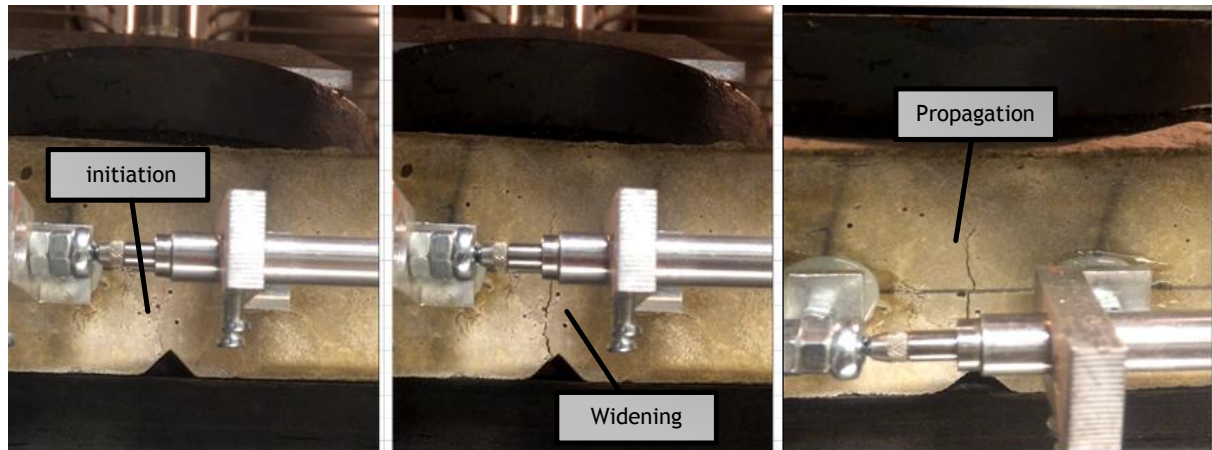

Figure 4-4 Crack initiation, widening and propagation from the tip of the notch

4.4.1 Monotonic loading test results

(Figure 4-5) shows a typical failure of plain concrete and geogrid sample. All plain concrete replicates followed the same failure where cracks reached the top surface to cause total failure. Whereas, all geogrid samples did not fail completely, the cracks did not reach the top surface of the slab.

(Figures 4-6 a, b &c) show the applied load versus the average crack mouth opening displacement of each set of replicates separately. After the application of loading, two phases were encountered the pre-cracking and post-cracking phase separated by an initial cracking point. In the pre-cracking phase, as shown in (figure 4-7) that the CMOD values in the geogrid reinforced samples are higher than the plain concrete and the initial cracking always occurs before (6.03 KN for geogrid and 8.36 KN for plain concrete). Placing the

geogrid at one third the thickness divides the overlay into two layers: upper and lower layer. The loss in flexure strength between the plain and geogrid reinforced samples is due to the slippage at the interface between geogrid and concrete. An FEM model was developed for the upper layer of the overlay which has a thickness of 35 mm showed that the force required to cause failure of the overlay is 5.96 KN which is almost the same failure load of the geogrid reinforced sample.

After the initial cracking, for both plain and reinforced concrete, a sudden and significant increase in CMOD was witnessed. Then the crack started widening and propagating upwards. It is noticed from the (figure 4-8), which is the average data for the three replicates, that rate of crack opening in the plain concrete is higher than the geogrid reinforced one. For example, at a load of 20 KN the CMOD values of plain and reinforced concrete are 0.7 and 0.43 mm respectively, which means 38.5% decrease in the CMOD. The load is redistributed to the geogrids after initial cracking of concrete; therefore the resistance against crack opening in the geogrid sample will be higher than plain concrete resulting in smaller values of CMOD.

The machine limit for monotonic loading is between 23-24 KN which is the end point of the test. After test completion, it was noticeable that all plain concrete samples experienced complete failure; however, in geogrid reinforced samples the crack did not even reach the top of the specimen. This is also shown from the substantial values of CMOD in plain concrete, which means the crack width was wide enough to propagate and reach the top to cause total failure. Unlike geogrid reinforced sample where cracks could not propagate to reach the top.
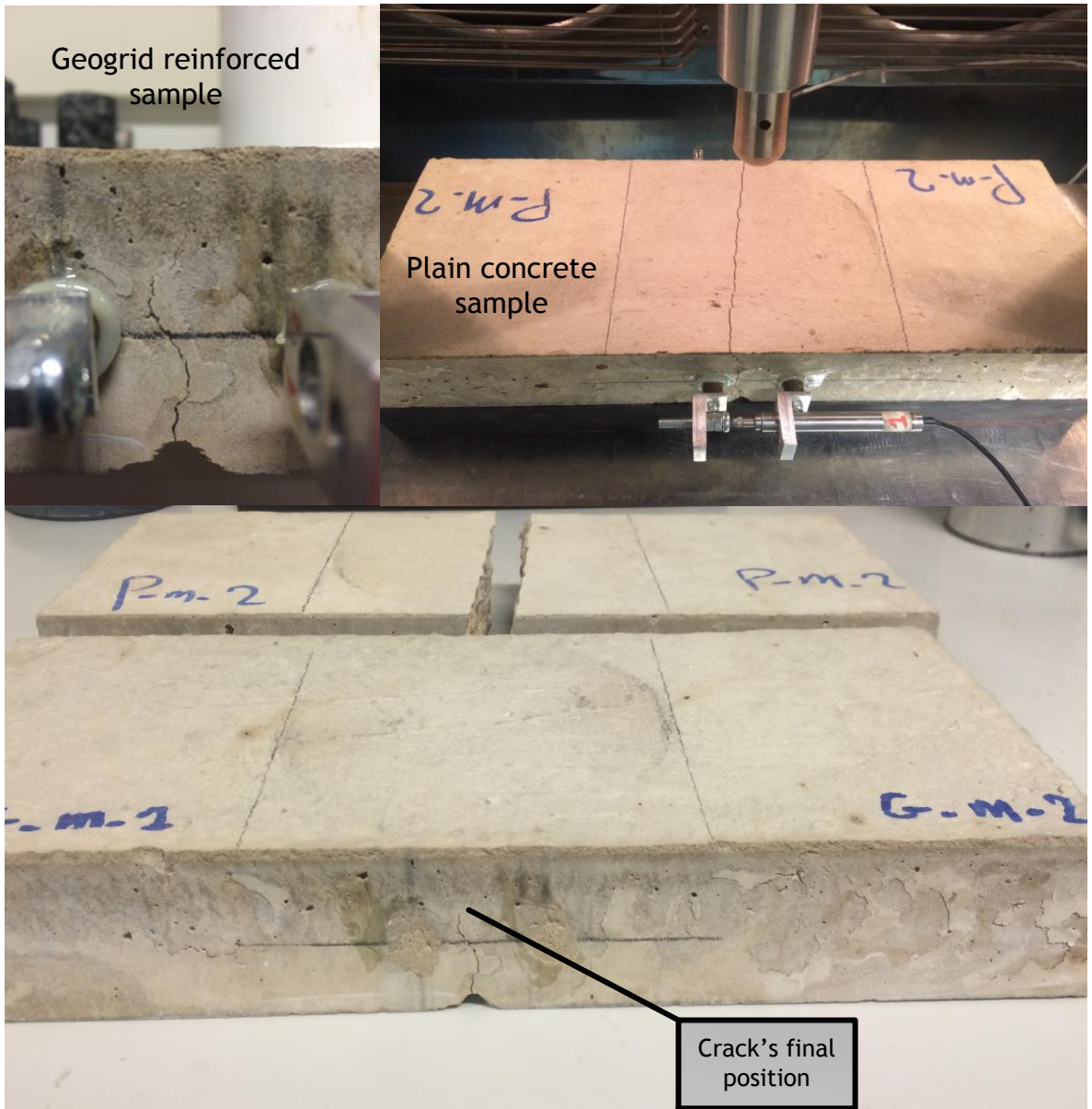
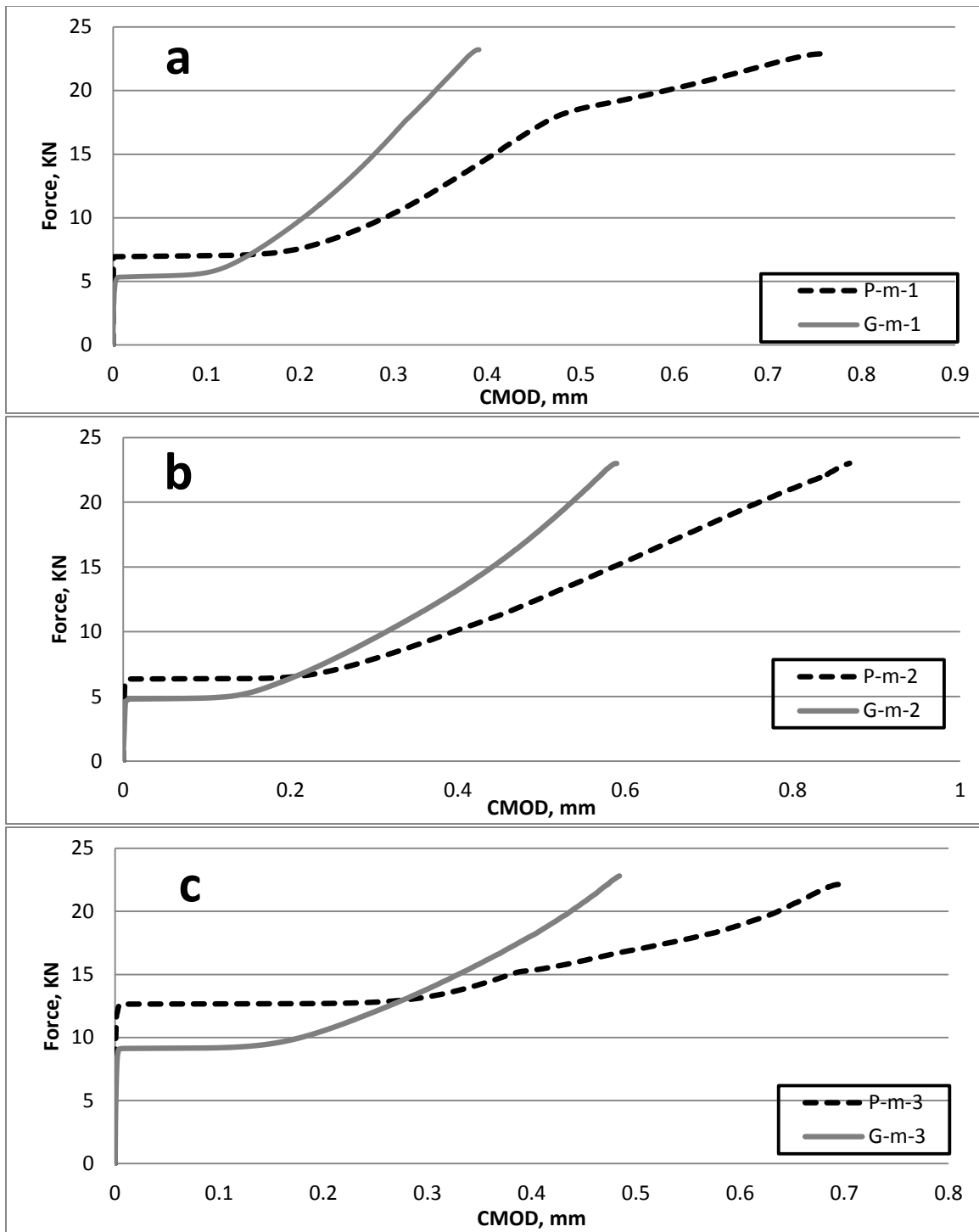Figure 4-5 Plain Vs reinforced concrete failure mode under monotonic loading

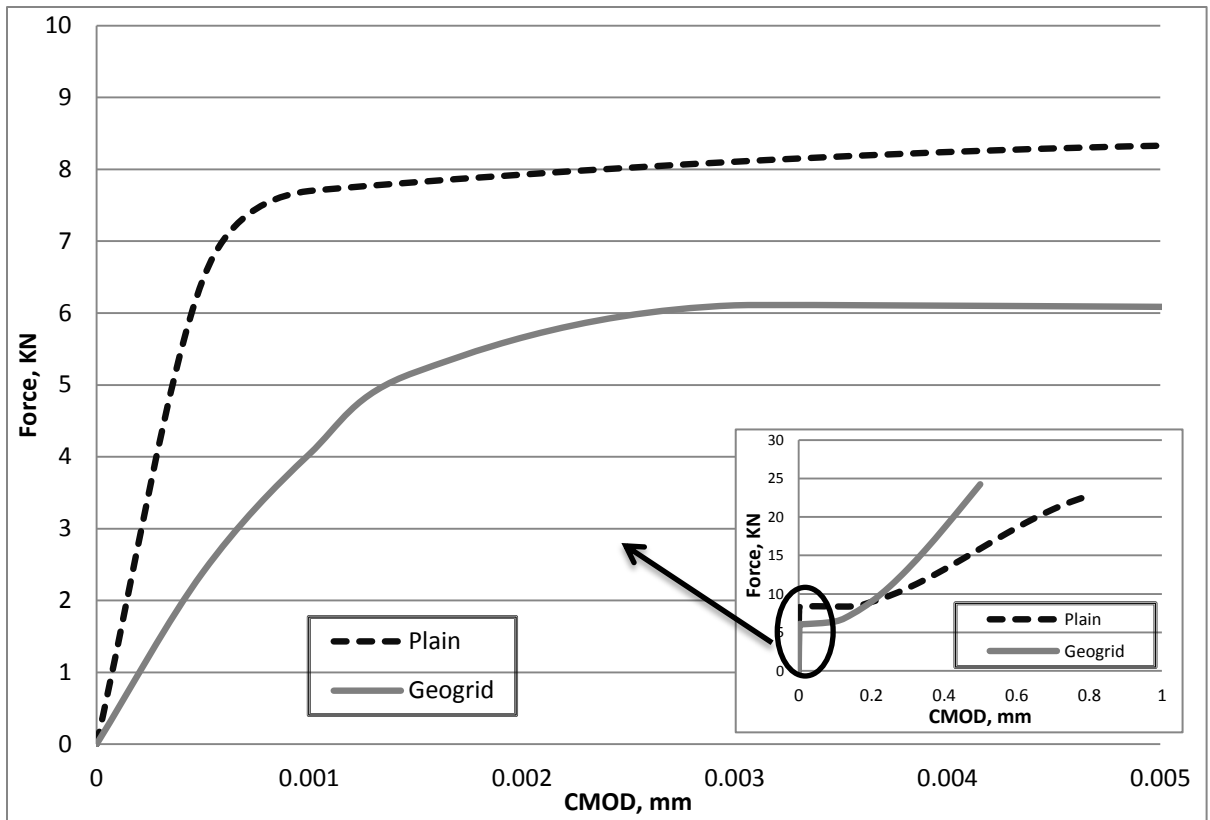Figure 4-6 Force versus crack mouth opening displacement for each set of replicates under monotonic loading

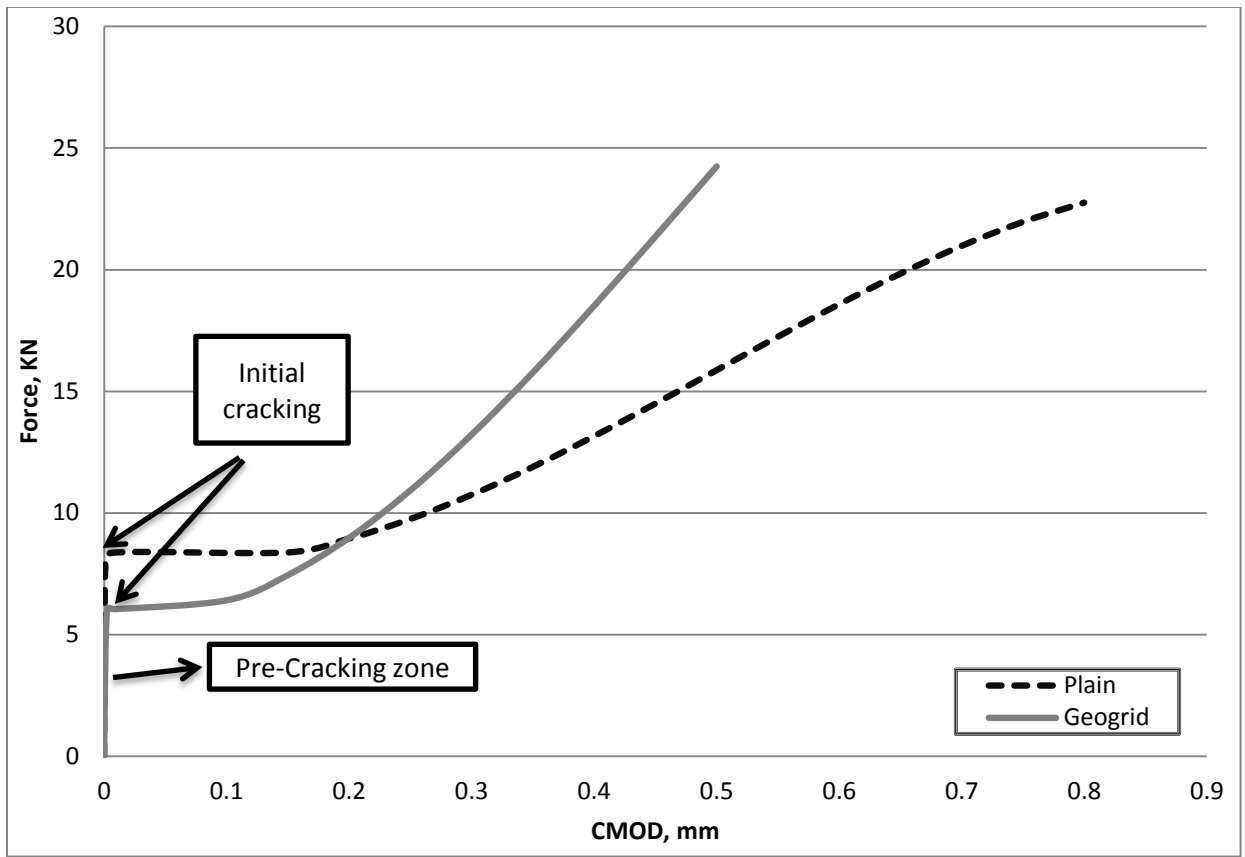Figure 4-7 Average force versus CMOD for the pre-cracking phase

Figure 4-8 Average force versus CMOD for the plain and geogrid reinforced concrete

4.4.1.1 FE model calibration

The results from the experimental work were used to calibrate the FE models for later use
and investigation as shown in (figure 4-9). First the concrete model was calibrated to get
the properties of concrete. After that these properties were used in the calibration of the
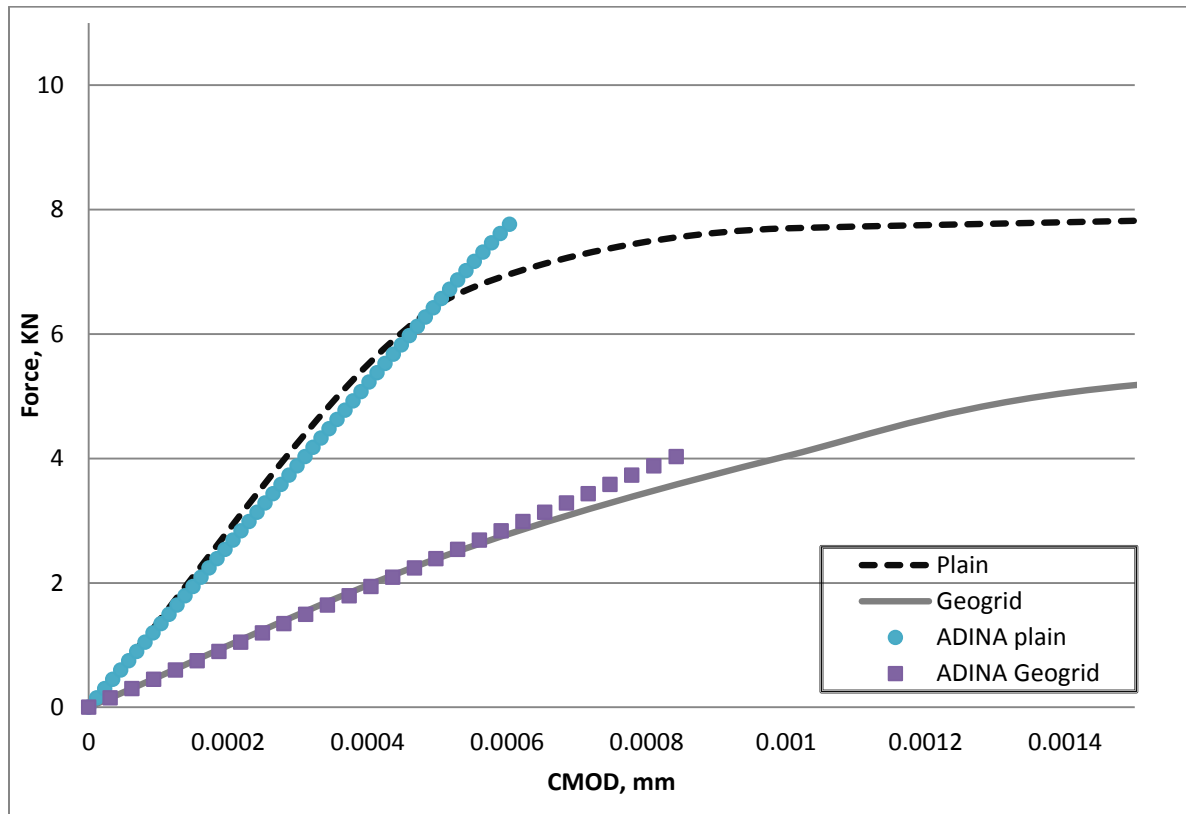geogrid concrete model.

Figure 4-9 Finite element model calibration

Some sensitivity analysis was done to see the significance of the geogrid layer location in
the overlay. Four FEM models were made to investigate this task; the first one is plain
concrete sample subjected to flexural loading, the other ones are reinforced with geogrid at
different locations: 1/3 h, 1/5 h and 1/8 h. The analysis was done for the pre-cracking zone.

It was noticed from the figure 4-10 that the capacity of the section increases as the geogrid layer is placed near the bottom of the overlay, which is predictable since the depth of the upper layer of the overlay is increasing. On the other hand, the stiffness of the reinforced specimens is not varying too much. It is worthy to mention that the plain concrete model is the stiffest among all of them. For the ease of construction of thin concrete overlays, placing the goegrid layer at one third the depth is a practical choice.
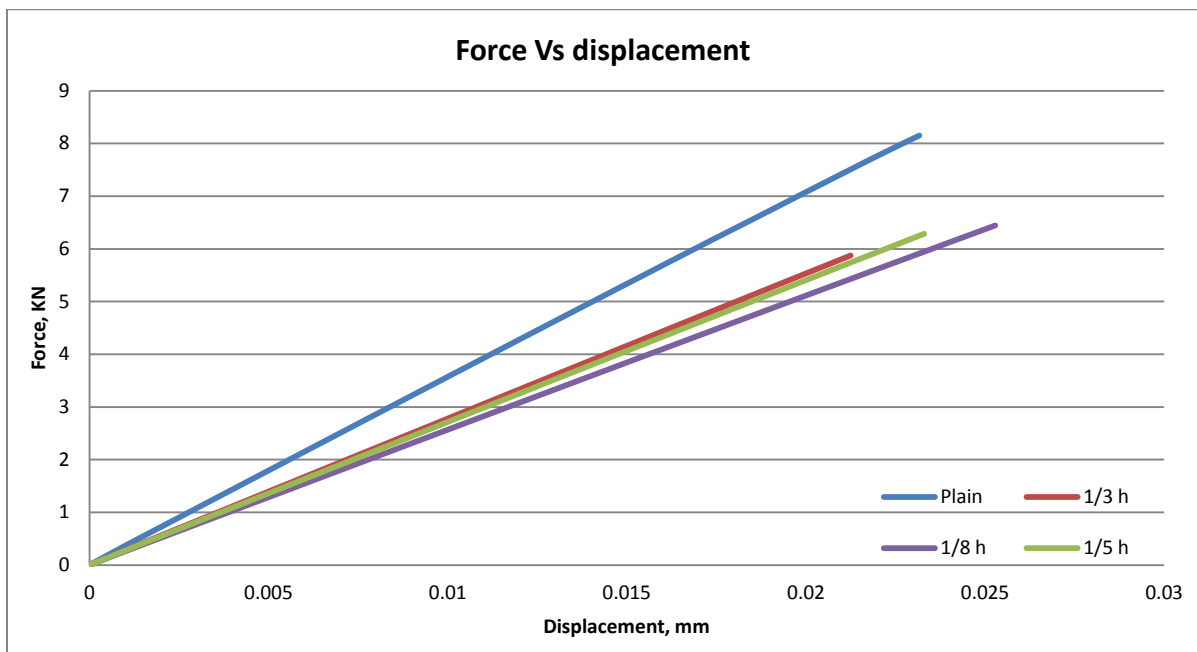

Figure 4-10 Geogrid layer position sensitivity analysis

4.4.2 Cyclic loading testing

The procedure followed in this test is to apply the maximum number of cycles the machine can perform which is 10 sweeps each is 10000 cycles. During testing, the crack was visually monitored and the termination point of the test was when the crack reaches the top of the specimen. The frequency of the load is 10 Hz and no rest period was specified between each cycle. So the time needed to complete 100000 cycles is 2 hours and 47 minutes.

(Figure 4-11) shows the average value of the crack opening measured for each specimen depending on the number of load cycles. During the testing of plain concrete samples, it has been observed that a crack was initiated from the tip of the notch and grew in length and width until reaching the top of the specimen and the average number of cycles responsible for total failure is 32328 cycles. Whereas, for geogrid reinforced samples the crack did not reach the top of the specimen even after 100000 cycles. This means that the geogrid has delayed the crack propagation and extended the life of the sample at least from 32328 to 100000 cycles.

During the first cycles of loading, it was noted that the geogrid reinforced samples cracked before the plain concrete. However, after initial cracking, the plain concrete samples showed a big jump in the crack opening unlike the geogrid reinforced samples which is less in magnitude (figure 4-12).

(Figure 4-13) shows a typical failure of plain concrete and geogrid sample. All plain concrete replicates followed the same failure where cracks reached the top surface to cause

total failure. Whereas, all geogrid samples did not fail completely, the cracks did not reach
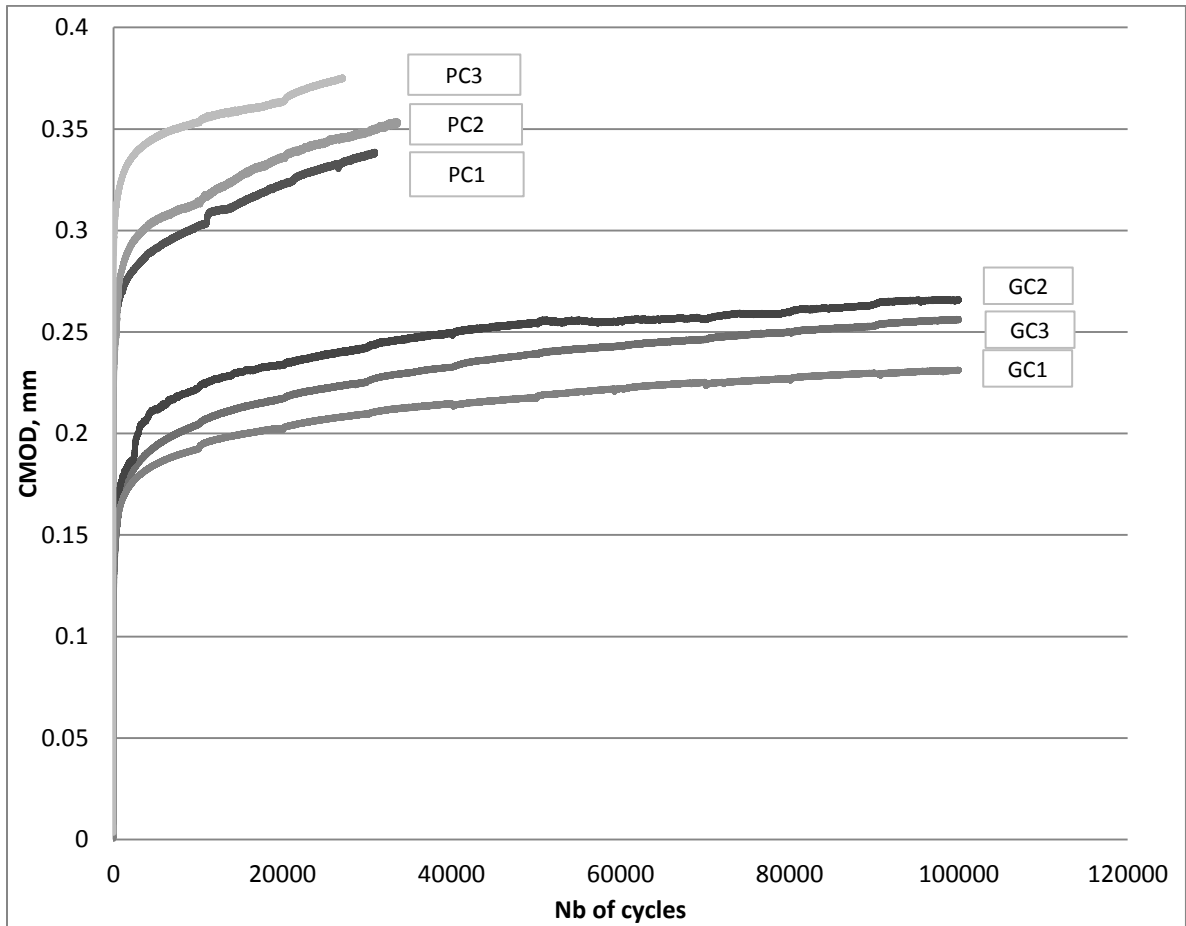
the top surface of the slab.

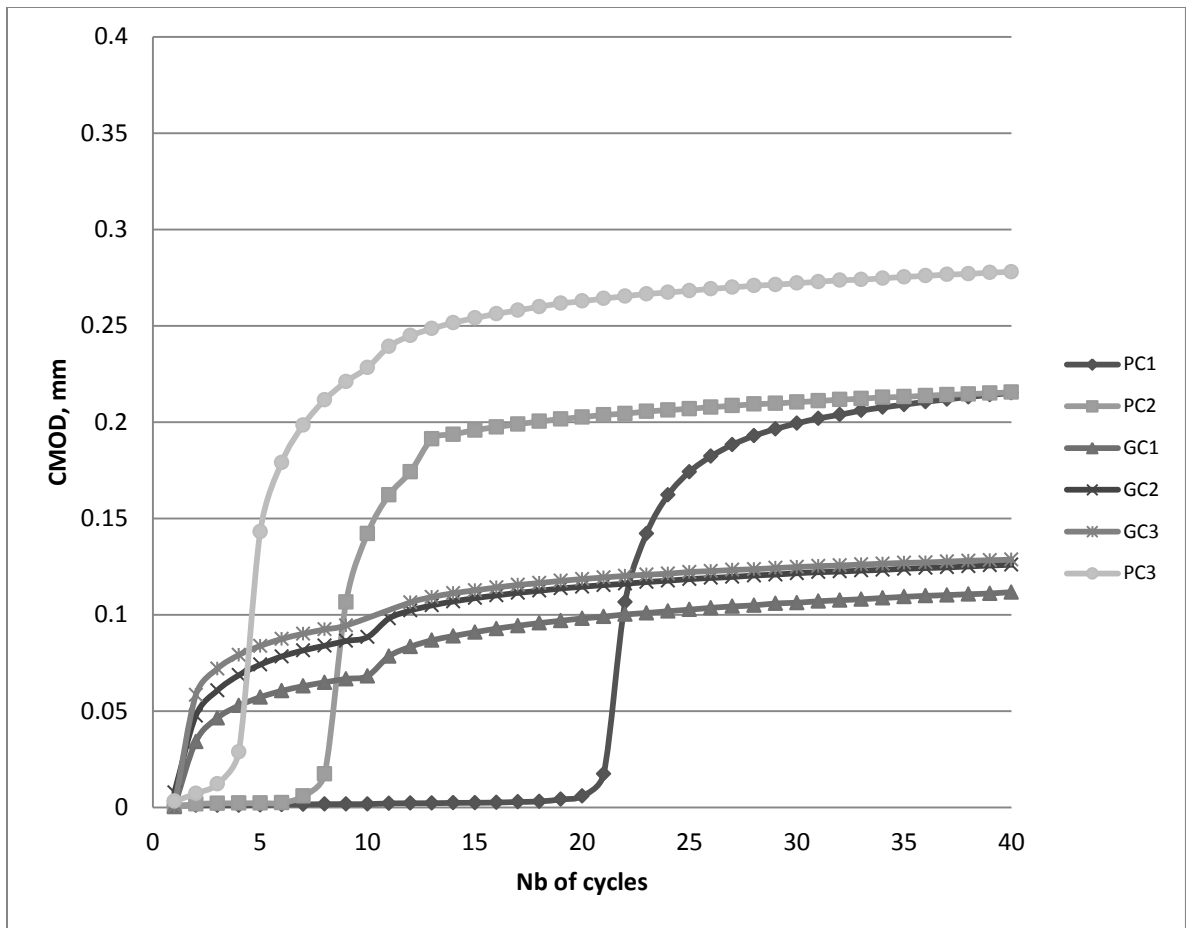Figure 4-11 CMOD versus number of cycles for each specimen

Figure 4-12 CMOD versus number of cycles for each specimen in the pre-cracking phase
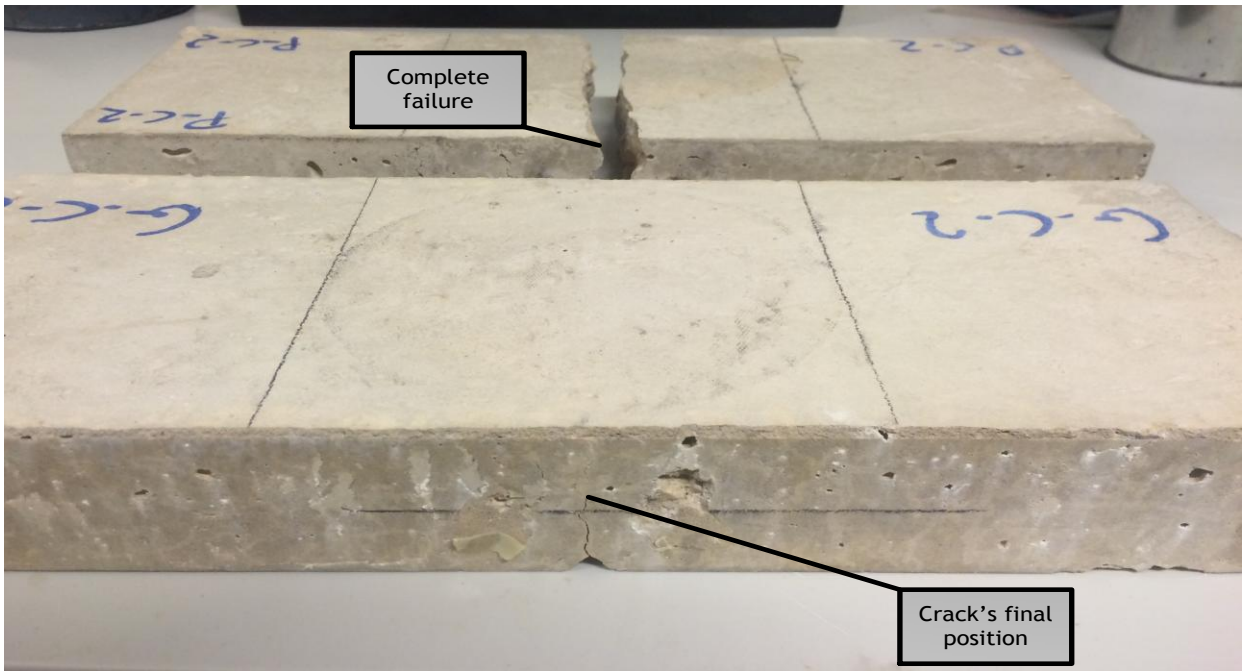
Figure 4-13 Plain versus geogrid reinforced concrete failure mode under cyclic loading

CHAPTER 5

CONCLUSIONS AND FUTURE WORK

5.1 Conclusions

This research study investigated the use of geogrid as main reinforcement in thin concrete overlays. This project study the effect of placing geogrid in the overlays under the condition of mode I cracking (tension and bending). Plain and reinforced Portland cement concrete samples with the same mix design were tested under direct tension monotonic loading and under flexure monotonic/cyclic loading. Based on the findings from all tests, the benefits of the inclusion of the geogrid in concrete overlays can be summarized as follows:

- Different failure modes were observed for specimens under direct tension. Plain samples exhibited brittle failure however the geogrid reinforcement adds a substantial post-cracking ductility where reinforced sample showed an increase in strength after cracking as well as large deformation

- In terms of fracture energy, the reinforced samples were more resilience to cracking than the plain concrete ones

- The used geogrid is considered stiff geogrid. The stress strain curve obtained from the tension testing of geogrids showed that this material is a Multi-linear elastic-plastic. However, in pavements (at low strains) the geogrid material can be modeled as isotropic linear elastic

- Slabs tested under monotonic loading showed that the inclusion of geogrids results in early initial cracking and the values of CMOD of the geogrid samples in the pre-cracking phase are greater than the plain concrete. However, after initial cracking the geogrid controls the rate of crack opening; where in plain concrete samples the CMOD values are much higher than the reinforced sample

- Two different modes of failure were observed for the slab samples under monotonic loading. The plain concrete samples completely failed and split in half whereas the crack in the geogrid samples did not reach the top face of concrete.

- Slabs tested under cyclic loading showed that the inclusion of geogrids results in substantial improvement in the performance and service life of the overlays in terms of the required number of cycles for failure and crack opening/propagation

5.2 Future work

The inclusion of geogrid in concrete overlay under mode I cracking reveals significant improvement in the behavior and performance of the overlay. In the future, mode II cracking, the sliding mode, which results from traffic loading and causes in-plane shear should be investigated.

Placing the geogrid in the concrete overlay at any depth forces the contractors to pour the concrete in two separate layers and each layer should be vibrated. Therefore, extra cost can be encountered and this point needs investigation.

The subgrade is replaced in the flexure test by neoprene rubber pad. For future testing this pad can be divided into two parts leaving a gap in the middle. This will ensure a good support for the overlay but also will help the specimen to move more when the load is applied allowing further crack propagation.

BIBLOGRAPHY

Abdelhalim, A. O., 1983. *Geogrid Reinforcem ent o f Asphalt Pavements.* Ontario: University of Waterloo.

ADINA, 2012. *Theory and Modeling Guide Volume I: ADINA,* Watertown, MA: ADINA R& D, Inc.

Aldea, C. M. & Darling, J. R., 2004. *Effect of Coating on Fiberglass Geogrid Performance.* Limoges, France, s.n.

Al-Qadi, I. L. et al., 2008. *Synthesis on Use of Geosynthetics in Pavements and Development of a Roadmap to Geosynthetically-Modified Pavements,* s.l.: Federal Highway Administration.

Barksdale, R., Brown, S. & Chan, F., 1989. Potential Benefits of Geosynthetics in Flexible Pavement Systems. *Transportation Research Board,* Volume National Cooperative Highway Research Program Report No. 315, p. 56.

Barksdale, R. D., 1991. *Fabrics in Asphalt Overlays and Pavement Maintenance,* Washington, DC: National Research Council.

Burd, H. & Brocklehurst, C., 1990. Finite Element Studies of the Mechanics of Reinforced Unpaved Roads. *Proceedings of the Fourth International Conference on Geotextiles, Geomembranes and Related Products,* Volume 1, pp. 217-221.

Burd, H. & Brocklehurst, C., 1992. Parametric Studies of a Soil Reinforcement Problem Using Finite Element Analysis. *Proceedings of the International Conference on Computer Methods and Advances in Geomechanics,* Volume 3, pp. 1783-1788.

Burd, H. & Houlsby, G., 1986. A Large Strain Finite Element Formulation for One Dimensional Membrane Elements. *Computers and Geotechnics,* Volume 2, pp. 3-22.

Button, J. W. & Lytton, R. L., 1987. *Evaluation of fabrics, fibers and grids in overlays.* Ann Arbor, MI, s.n., pp. 925-934.

Cleveland, G. S., Button, J. W. & Lytton, R. L., 2002. *Geosynthetics in Flexible and Rigid Pavement Overlay Systems to Reduce Reflection Cracking,* Texas: Report No. FHWA/TX-02/1777-1.

CPTP, 2007. *Early-Entry Sawing of Portland Cement Concrete Pavements,* s.l.: Federal Highway Administration Office of Pavement Technology.

De Bondt, A. H., 1998. *Anti-Reflective Cracking Design of (Reinforced) Asphalt Overlays.* Delft: Delft University of Technology.

Dhule, S. B., Valunjkar, S., Sarkate, S. & Korrane, S., 2011. Improvement of Flexible Pavement With Use of Geogrid. *Electronic Journal of Geotech Engineering,* pp. 269-279.

Dondi, G., 1994. Three-Dimensional Finite Element Analysis of a Reinforced Paved Road. *Proceedings of the Fifth International Conference on Geotextiles, Geomembranes and Related Products,* Volume 1, pp. 95-100.

EL Meski, F. & Chehab, G., 2014. Flexural Behavior of Concrete Beams Reinforced with Different Types of Geogrids. *Journal of materials in civil engineering,* 26(8).

Gonzalez-Torre, I., Calzada-Perez, M., Vega-Zamanillo, A. & Castro-Fresno, D., 2015. Evaluation of reflective cracking in pavements using a new procedure that combine loads with different frequencies. *Construction and Building Materials ,* Issue 75, pp. 368-374.

Harrington, D. et al., 2007. *Guide to Concrete Overlay Solutions,* s.l.: National Center for Concrete Pavement Technology (CP Tech Center), Iowa State University.

Huang, Y. H., 1993. *Pavment analysis and design.* 2nd ed. s.l.:Prentice Hall.

ISU, 2004. *Concrete paving workforce eference No. 3: concrete pavement joint sawing,cleaning, and Seali6ng.,* Ames: Center for Portland Cement Concrete Pavement Technology, Iowa State University (ISU).

Khodaii, A. & Fallah, S., 2009. Effects of geosynthetic reinforcement on the propagation of reflection cracking in asphalt overlays. *Int. J. Civ. Eng.,* Volume 7(2), p. 131–140.

Kim, H., 2007. *Investigation of Toughening Mechanisms in the Facture of Asphalt Concrete using the clustered Discrete Element Method.* s.l.:University of Illinois at Urbana-Champaign.

Kim, J. & Buttlar, W. G., 2002. Analysis of reflective crack control system involving reinforcing grid over based-isolating interlayer mixture. *Journal of Transportation Engineering (ASCE),* p. 375–384.

Kim, J. J. & Taha, M. R., 2014. Experimental and Numerical Evaluation of Direct Tension Test for Cylindrical Concrete Specimens. *Hindawi Publishing Corporation Advances in Civil Engineering,* pp. Volume 2014, Article ID 156926, 8 pages.

Kim, Y. K. & Lee, S. W., 2013. Performance evaluation of bonded concrete overlay. *Elsevier Ltd,* pp. 464 - 470.

Koerner, R. M., 1994. *Designing with Geosynthetics.* Third Edition ed. Upper Saddle River, NJ: Prentice Hall.

Kuo, C.-M. & Hsu, T.-R., 2003. Traffic Induced Reflective Cracking on Pavements with Geogrid-Reinforced Asphalt Concrete Overlay. *82th Annual TRB Meeting,* pp. 1-23.

Kwon, J. & Tutumluer, E., 2009. Geogrid Base Reinforcement with Aggregate Interlock and Modeling of Associated Stiffness Enhancement in Mechanistic Pavement Analysis. *Journal of the Transportation Research Board,* Volume 2116, pp. 85-95.

Lytton, R. L., 1989. Use of Geotextiles for Reinforcement and Strain relief in Asphalt Concrete. *Geotextiles and Geomembranes vol.8,* pp. 217-237.

Maxwell, S., Kim, W., Edil, T. B. & Benson, C. H., 2005. *Effectiveness of geosynthetics in stabilizing soft subgrades,* Madison, WI: s.n.

Miura , N., Sakai, A., Taesiri, Y. & Yamanouchi, T., 1990. Polymer Grid Reinforced Pavement on Soft Clay Grounds. *Geotextiles and Geomembranes,* Volume 9, pp. 99-123.

Monismith, C. L. & Coetzee, N. F., 1980. *Reflection cracking: analysis, laboratory studies and design considerations.* Louisville, KY, s.n., pp. 268-313.

Nawy, E. G., 2000. *Reinforced concrete: A Fundamental Approach.* New Jersey : Prentice Hall.

Palmeira, E. M. et al., 2008. Geosynthetics Materials and Applications for Soil Reinforcement and Enviromental Protection Works. *Electronic Journal of Geotehnical Engineering,* 13(Special Issue State of the Art in Geotechnical), pp. 1-38.

Rajeshkumar, K., Mahendran, N. & Gobinath, R., 2010. Experimental Studies on Viability of Using Geosynthetics as Fibers in Concrete. *International Journal of Applied Engineering Research,* pp. 15-28.

Rigo, J. M., 1993. *General introduction, main conclusions of 1989 conference on reflective cracking in pavements, and future prospects.* Liege, Belgium, E & FN Spon, pp. 3-20.

Roberts, F. L., Kandhal, P. S., Brown, E. R. & Lee, D. Y., 1996. *Hot Mix Asphalt Materials, Mixture Design and Construction.* Lanham, Maryland: NAPA Research and Education Foundation.

Ruiz, J. M. et al., 2001. Concrete Temperature Modeling and Strength Prediction Using Maturity Concepts in the FHWA HIPERPAV Software. *Transportation Research Board.*

Saito, M. & Imai, S., 1983. Direct Tensile Fatigue of Concrete By the Use of Friction Grips. *ACI Journal ,* pp. 431-437.

Smith, K. D., Yu, H. T. & Peshkin, D. G., 2002. *Portland Cement Concrete Overlays: State of the Technology Synthesis,* Washington, DC: Federal Highway Administration.

Suprenant , B. A., 1995. *Sawcutting Joints in Concrete,* s.l.: The AberdeenGroup.

Swaddiwudhiponga, S., Lu, H.-R. & Wee, T.-H., 2003. Direct tension test and tensile strain capacity of concrete at early age. *Cement and Concrete Research,* Volume 33, p. 2077–2084.

Tang, X., Kim, S. & Chehab, G. R., 2008. *Laboratory Study of Geogrid Reinforcement in Portland Cement Concrete.* Chicago, Illinois, USA, s.n., pp. 769-778.

Taylor, P. C., Kosmatka, S. H. & Voigt, G. F., 2007. *Integrated Materials and Construction Practices for Concrete Pavement: A State-of-the-Practice Manual,* Ames: National Concrete Pavement Technology Center/ Center for Transportation Research and Education Iowa State University.

Wathugala, G., Huang, B. & Pal, S., 1996. Numerical Simulation of Geosynthetic Reinforced Flexible Pavement. *Transportation Research Record,* Volume 1534, pp. 58-65.

Xie, N. & Liu, W., 1989. Determining Tensile Properties of Mass Concrete by Direct Tensile Test. *ACI Materials Journal,* pp. 214-219.

Zheng, W., Kwan, A. & Lee, P., 2001. Direct Tension Test of Concrete. *ACI Materials jornal,* pp. 63-71.

Zornberg, J. et al., 2008. *Validating Mechanisms in Geosynthetic Reinforced Pavements,* Austin, Texas, USA: s.n.

Appendix A

Direct tension test procedure

The section below will explain the complete procedure followed in order to conduct the direct tension test.

A.1 First trial

At first some modifications were to be done in order to conduct the test on the "UTM-25" since it is mostly used for compression tests. Two steel plates were added to the base and actuator of the machine to fix the sample on them.

Samples with prismatic section were tested first. The ends of the specimen were glued with another two plates using epoxy and then bolted with the fixed plates as shown in figure A.1

A.1 testing setup of the first trial

However, this setup suffered from stress concentration at boundaries and localized failure at the interface between concrete and epoxy. Several steps were taken to avoid this failure like surface roughening, steel plate grooving, epoxy with higher strength bond and more curing time. But the problem still existed as shown in figure A.2. From there the use of new setup was needed.

A.2 Typical localized failure at the concrete/epoxy interface

A.2 FEM study

When the prismatic section failed and was no longer in use, new FEM trials were done in ADINA to process the tensile stress concentration in order to avoid the localized failure. The following are the studied samples:

1- Reduced section at the middle: this sample consists of two prismatic sections the first one is at boundaries and it is larger than the second one which is in the middle. The ends of the sample are glued with epoxy. It is found that this sample suffer from stress concentration at the end of the reduced section as shown in figure A.3.
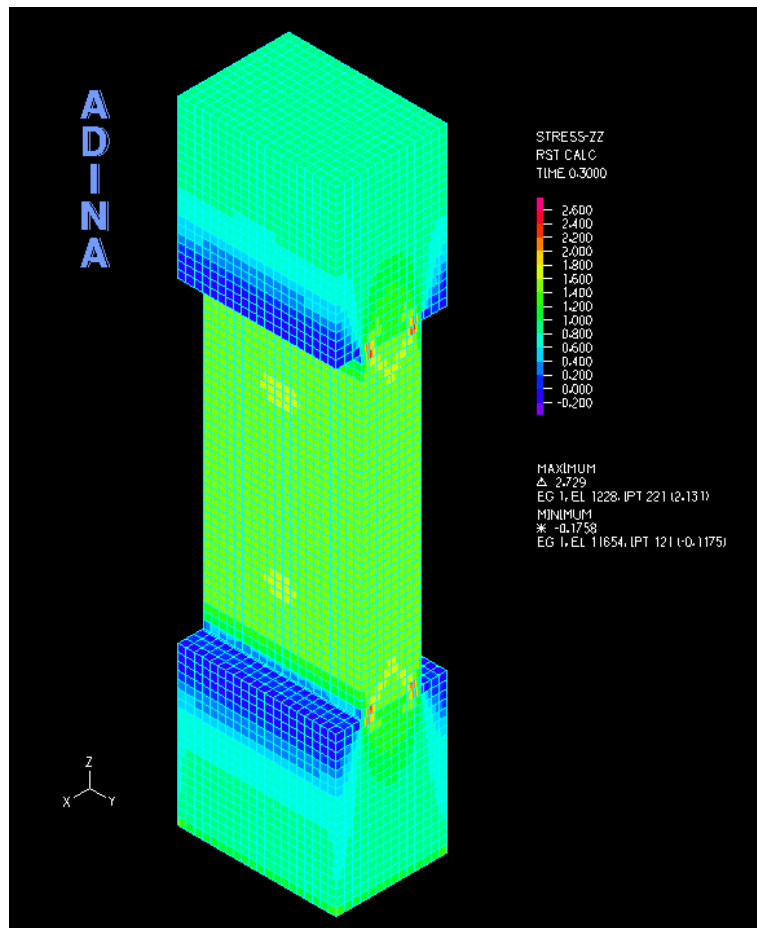
A.3 Reduced section at the middle

2- Gradually reduced section

A gradual reduction in the section was studied to see if the stress concentration at the ends can be eliminated, it was found that the stress at the start and end of the reduced section still high and would cause a localized failure as shown in figure A.4
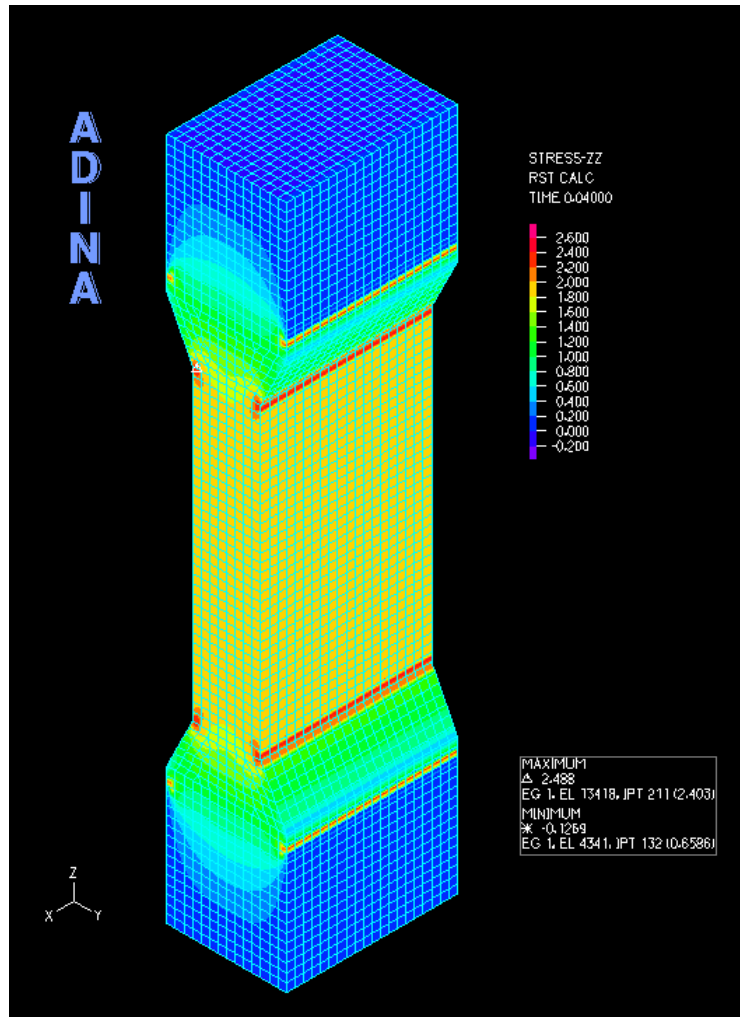
A.4 Gradually reduced section

3- The use of notch

The use of notch was found to be effective in inducing stress concentration at specific point as shown in figure A.5. Several shapes of notch were studied; the triangular notch is the most effective one in terms of inducing stress.
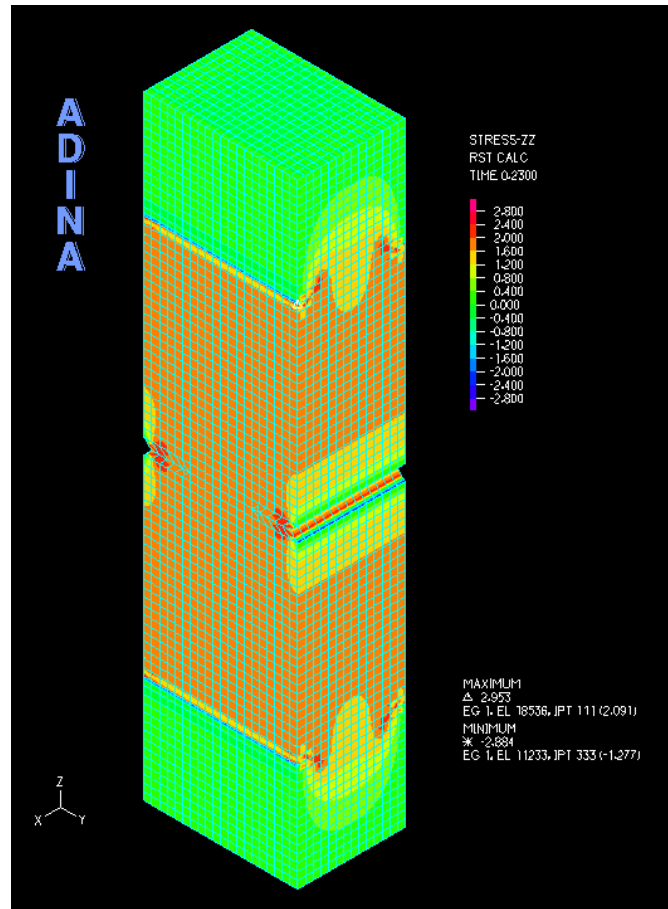
A.5 Notched sample

4- Elimination of the epoxy

The components of the epoxy glue are: hardener and resin. They should be added in a
specific ratio using a digital balance. This process should be done with high precision in
order to get the perfect mix. After that, the epoxy needs curing time which can be up to
24hrs depending on its type. In addition, it is not available here in Lebanon and should be
imported. All these factors are reasons to eliminate the glue from the process of fixing the
sample and start thinking about alternatives.

5- The usage of threaded rods

The idea of placing steel threaded rods in concrete turned out to be an effective way to apply tension load on the specimen in terms of simplicity and ease of installation. However, stress concentration developed around the rod. Therefore, it was decided to adopt a specimen with gradual reduction in thickness and with a notch in the middle of the specimen.

Several scenarios were considered for the analysis including one rod, two staggered rods and three staggered rods (figures A.6, A.7 & A.8). It was found that the only benefit of the staggered configuration is the increase of the net area at the section that passes through the steel rod. This area should be greater than any area along the length of the specimen to avoid localized separation.

A comparison was made between these configurations in terms of tensile stress distribution at a section where the strain is measured. The samples with staggered rods suffer from non-uniformity in stress distribution at that section as shown in figures A.7 & A.8. Whereas, more uniformity in stress in the section is noticed in the sample with one central rod.

On the other hand, another comparison was made to see the difference between sample with one rod and another with two rods (figures A.9 & A.10). It was found that the best configuration is the one with central rod. One more step was taken to decrease the stress concentration on the edge of the reduced section by increasing the length of the transition zone.
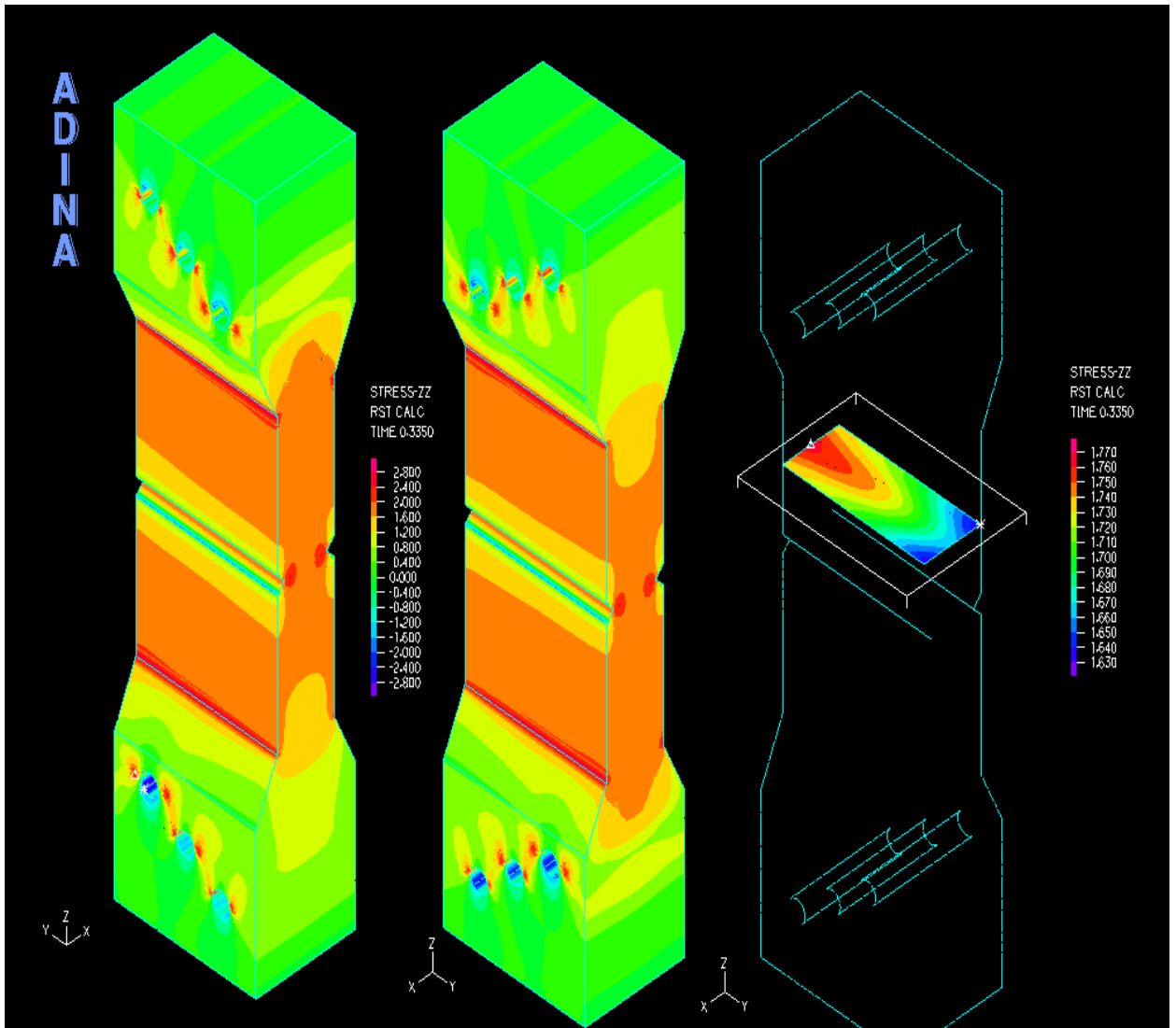
Eventually, the sample with one central rod is selected to be the best configuration. The net area at the section passing through the rod is A1=6020 mm^2 and the area at the middle of the sample is A2=2600 mm^2 (figure A.11)
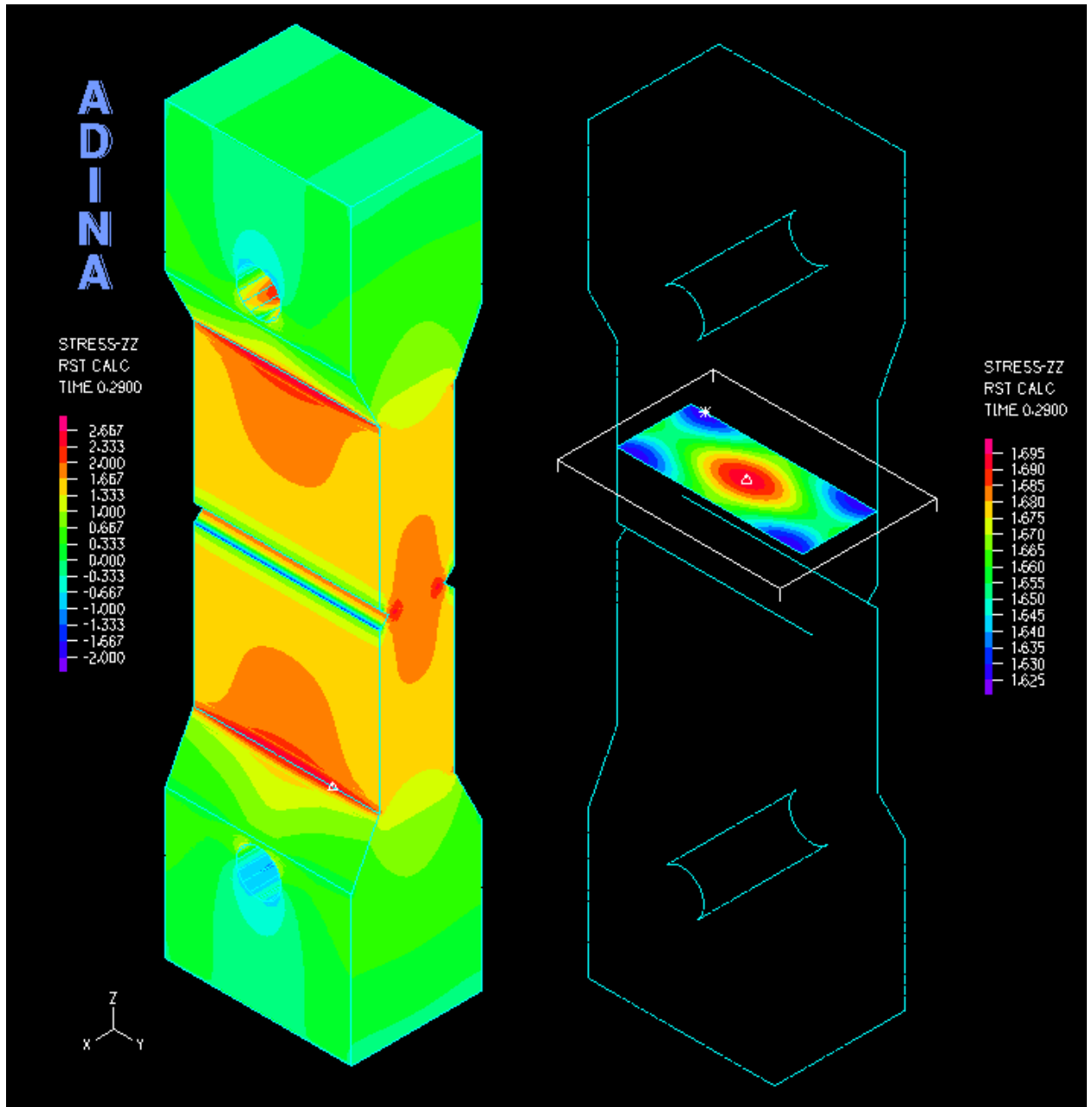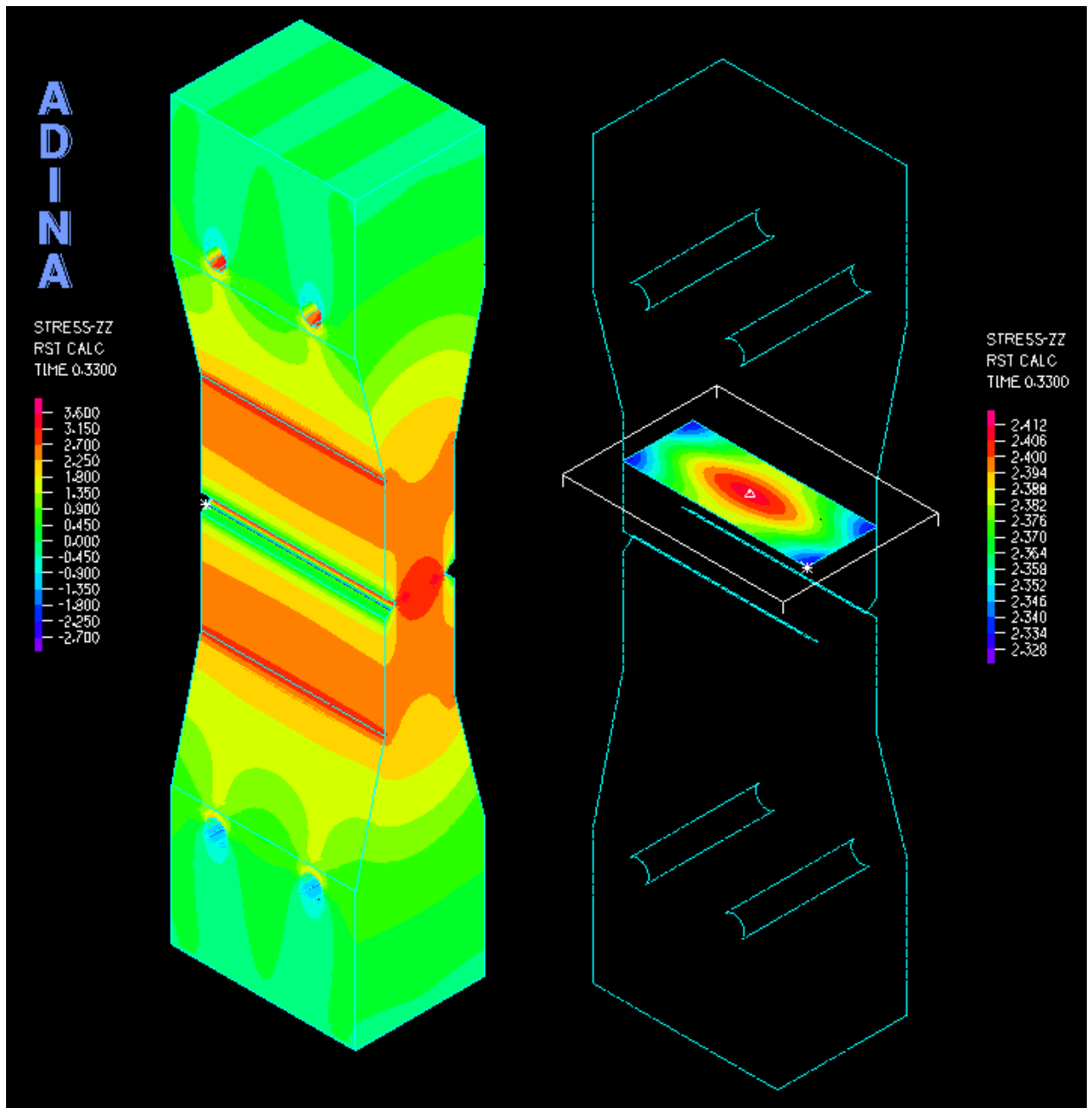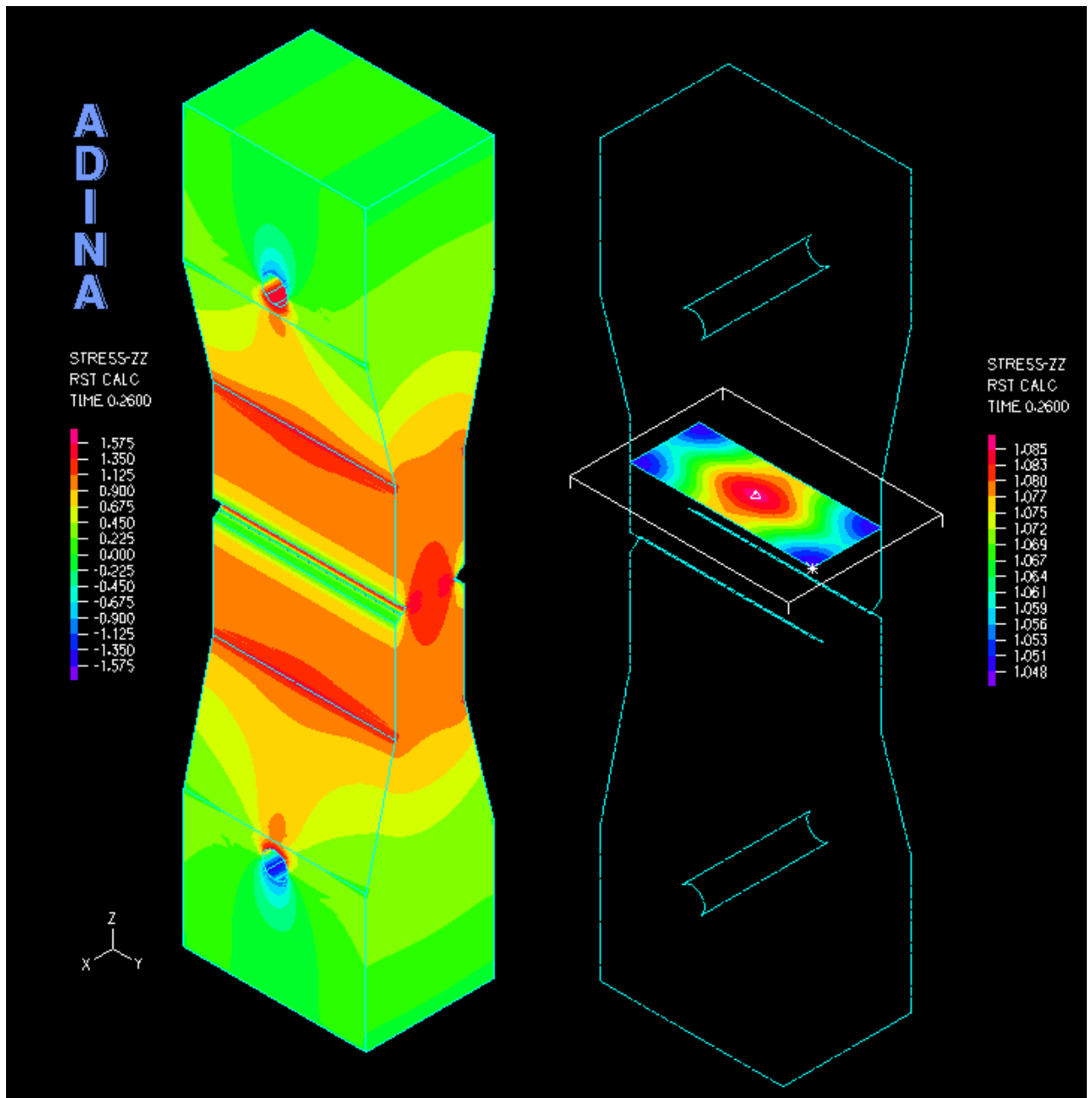

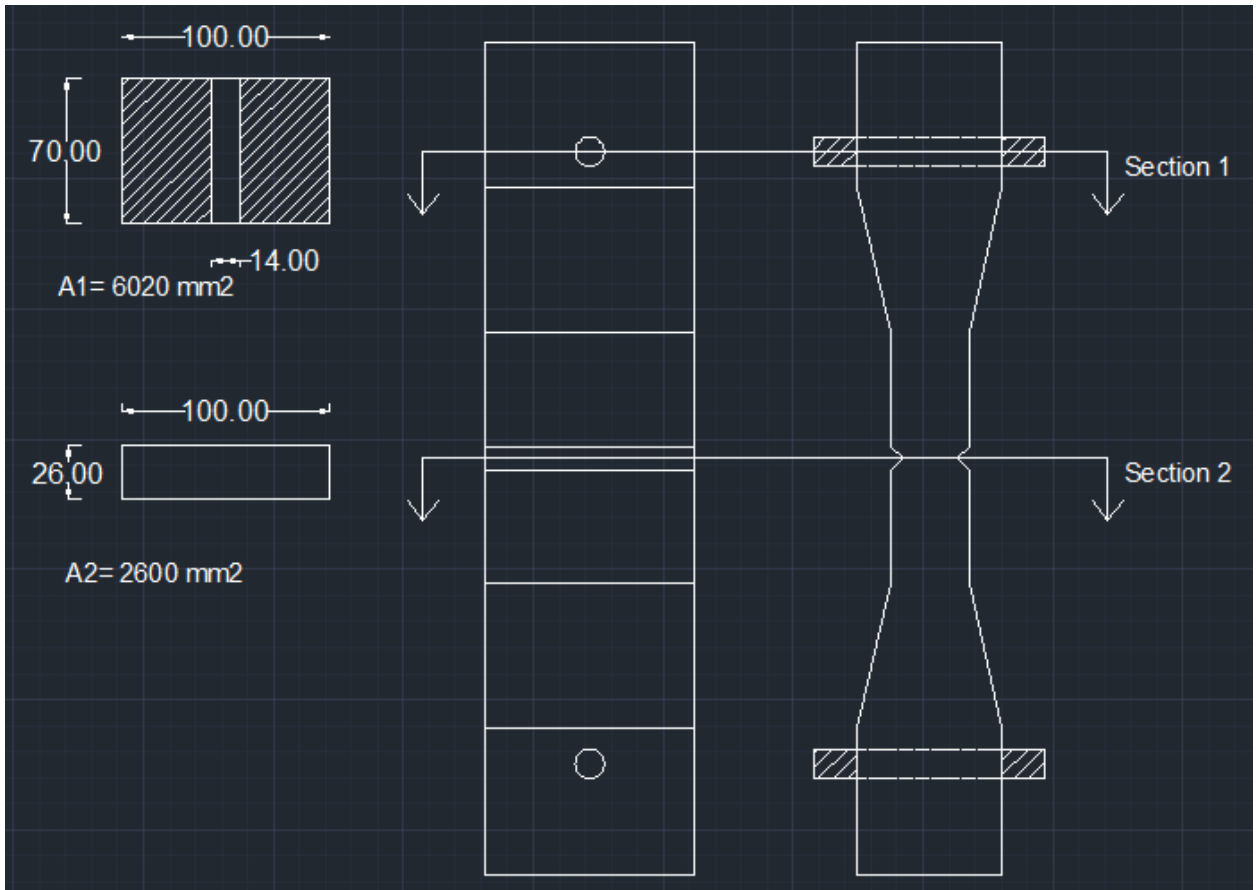A.6 Sample with one central rod
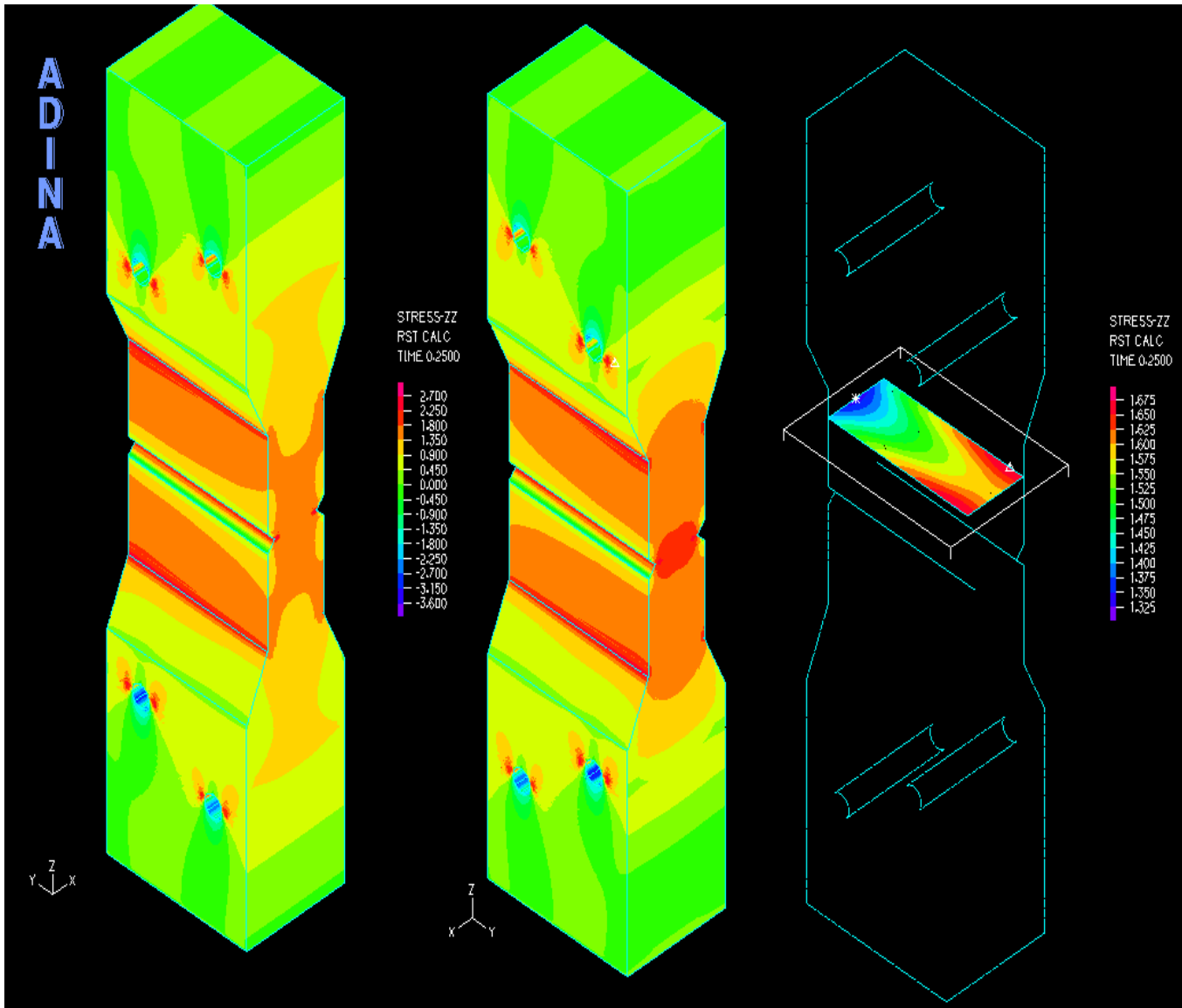
A.7 Sample with two staggered rods

A.8 Sample with three staggered rods

A.9 Sample with two rods

A.10 Adopted sample configuration

A.11 Difference in cross section area along the length of the sample

A.3 Materials preparation

1- Clean the sand from the large and unwanted particles by sieving

2- For this type of geogrids, the maximum aperture size= 11mm, the used aggregates were intermediate in size. Use the sieve #3/8 (9.5 mm) to eliminate any larger particles as shown in figure A.12. Clean the aggregates from dust and fine particles

A.12 Sieve #3/8

3- Place the sand and the gravels in the oven for 24 hours

4- Cut the geogrids, the best tool to do so is the metal cutting scissors

5- Weigh the materials as required in the design mix

A.4 Wooden molds

1- Prepare the wooden pieces as per required dimensions, the plywood thickness=16 mm it should be taken into consideration.

2- Glue the plexiglass notch on the inner sides of the molds by "Alteco" (figure A.13)

A.13 Gluing the notch

3- To make holes in the sides of the molds, put all the wooden pieces together and fix

them with vises to drill the holes. This step is very important to minimize the

manufacturing errors and to get uniform samples

4- Assemble the molds (figure A.14)

A.14 Assembled mold

A.5 Concrete casting/de-molding and curing

1- The use of high slump in the mix design for this type of small molds is preferable

2- Use steel rod and rubber hummer instead of vibrator, because the distance between the sides of the mold is relatively small

3- For de-molding, disassemble one side of the mold and gently push the sample out

4- Place the samples in a curing room

A.6 Sample preparation for testing

1- After curing, leave the samples in open air to dry from water

2- The strain was measured on the middle 10 cm of the specimen, so mark the centers of the targets with a pencil

3- Clean the sample (zones to be glued) and the targets in acetone for better bond

4- Use Devcon glue to glue the targets; make sure to mix the two liquids very well. The setting time of the used glue is 5 minutes and the curing time is a minimum of 1.5 hours

5- Install the end and side plates and tighten the screws. Make sure that the side plates are installed vertically and do not suffer from inclination

6- When you install the sample, make sure to attach the sample in the machine actuator first and then in the base, because the bottom plate has adjustable holes

A.7 The machine software

To conduct the direct tension test, use the stress strain software (UTS002 3.11). Define the test type as tensile loading (standard frame). Choose the type of loading, for displacement

control tests use the axial loading as actuator displacement. Make sure to insert test termination constraints like maximum actuator displacement and threshold load which is around 23 KN in the "UTM-25". Choose a text file logging rate, for such test 500 ms is convenient.

A.9 Data analysis

After test completion, the data is directly saved in the directory that you specify. The logging file contains: Time, axial force and axial displacement recorded from the LVDTs. The first reading of the LVDT is the last position of it, so subtract the initial value from all the readings. The average value of displacement is calculated from the LVDTs. Make sure that the readings from the LVDTs are recording almost similarly (figure A.15). This is a good indication and it means that the specimen is not tilting and it is perfectly aligned and as a result the load will be distributed uniformly over the area.
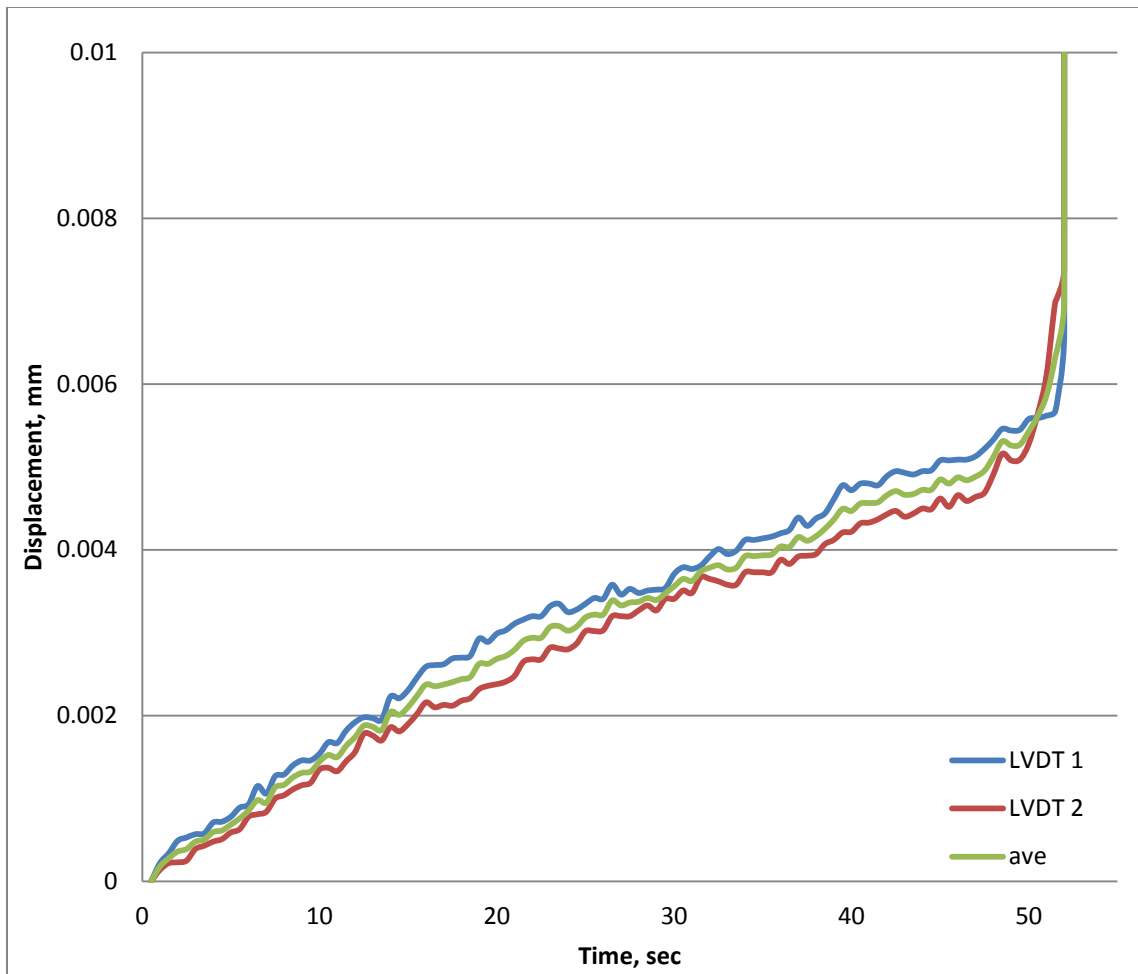
A.15 Graph showing the readings from two LVDT and their average

Appendix B

Flexure test procedure

The section below will explain the complete procedure followed in order to conduct the flexure test.

B.1 Geometry

The dimensions of the specimen should be based on the testing machine capacity and geometry. For the "UTM-25" the clear distance between the columns of the frame is 41 cm, thus it was decided to choose 38 cm to be the length of the sample. The width and the height of the sample as well as the compressive strength of the concrete were calculated based on the machine capacity which is 23- 24 KN, However, half of these values were considered in the design for the machine performance to be better since dynamic loading will also be applied.

B.2 Wooden molds and materials preparation

1- Prepare the wooden pieces as per required dimensions, the plywood thickness = 16 mm it should be considered in the calculation

2- Glue the plixglass notch on the base of the molds

3- Assemble the molds

4- The geogrid layer is placed at one third of the depth, so a line is marked on the sides of the mold from the inside using a correction pen

5- Cut the neoprene rubber as per required dimensions, the best tool to cut neoprene is the horizontal band saw used at high speed

6- Make sure that the steel plate is thick enough to ensure rigidity and to prevent plate deformation

7- Cut a layer of soft rubber to place it between the steel plate and the concrete sample, the best tool to cut soft rubber is cutter knife

8- Prepare all the materials for concrete casting (refer to appendix A)

B.3 Concrete casting/de-molding and curing
For more details about concrete casting and curing refer to Appendix A.

B.1 Concrete casting

B.2 No separation or major surface voids were observed after de-molding

B.4 Sample preparation for testing

7- After curing, leave the samples in open air to dry from water

8- The crack mouth opening displacement is measured on the middle 4 cm of the

specimen and 2 cm from the bottom, so mark the centers of the targets with a pencil

9- Clean the sample (zones to be glued) and the targets in acetone for better bond

10- Use Devcon glue to glue the targets; make sure to mix the two liquids very well.

The setting time of the used glue is 5 minutes and the curing time is a minimum of

1.5 hours

B.5 The machine software

To conduct the flexure test under monotonic loading, use the stress strain software

(UTS002 3.11). Define the test type as compressive loading (standard frame). Choose the

type of loading, for force control tests use the axial loading as axial force and define the

rate of loading. Make sure to insert test termination constraints like maximum actuator

displacement and threshold load which is around 23 KN in the "UTM-25". Choose a text

file logging rate, for such test 500 ms is convenient.

To conduct the flexure test under cyclic loading, use the dynamic modulus software

(UTS023 1.07b). Define the loading wave shape as haversine, specify the frequency of the

load and the number of cycles. The maximum number of sweeps in this software is 10

sweeps each is 10000 cycles. The UTM-25 is mostly used by the asphalt students, some

modifications should be made on the tuning parameters of the dynamic modulus test such

as PID curve. The PID curve define the shape of the wave, if not changed it won't take the

correct shape of the haversine. The PID curve for the concrete material is for Proportional=

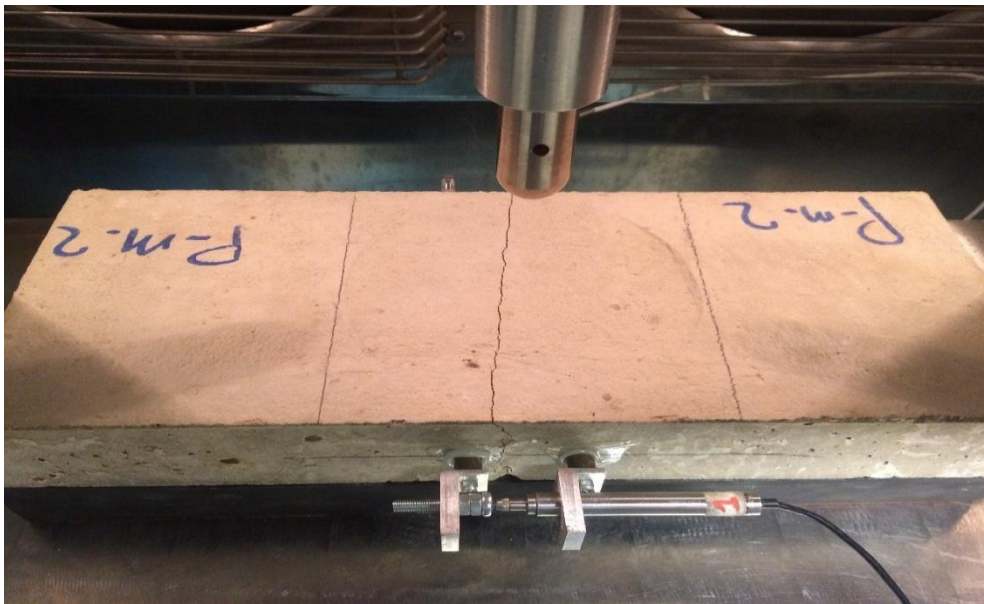5000, Integral= 10 and Derivative= 1200
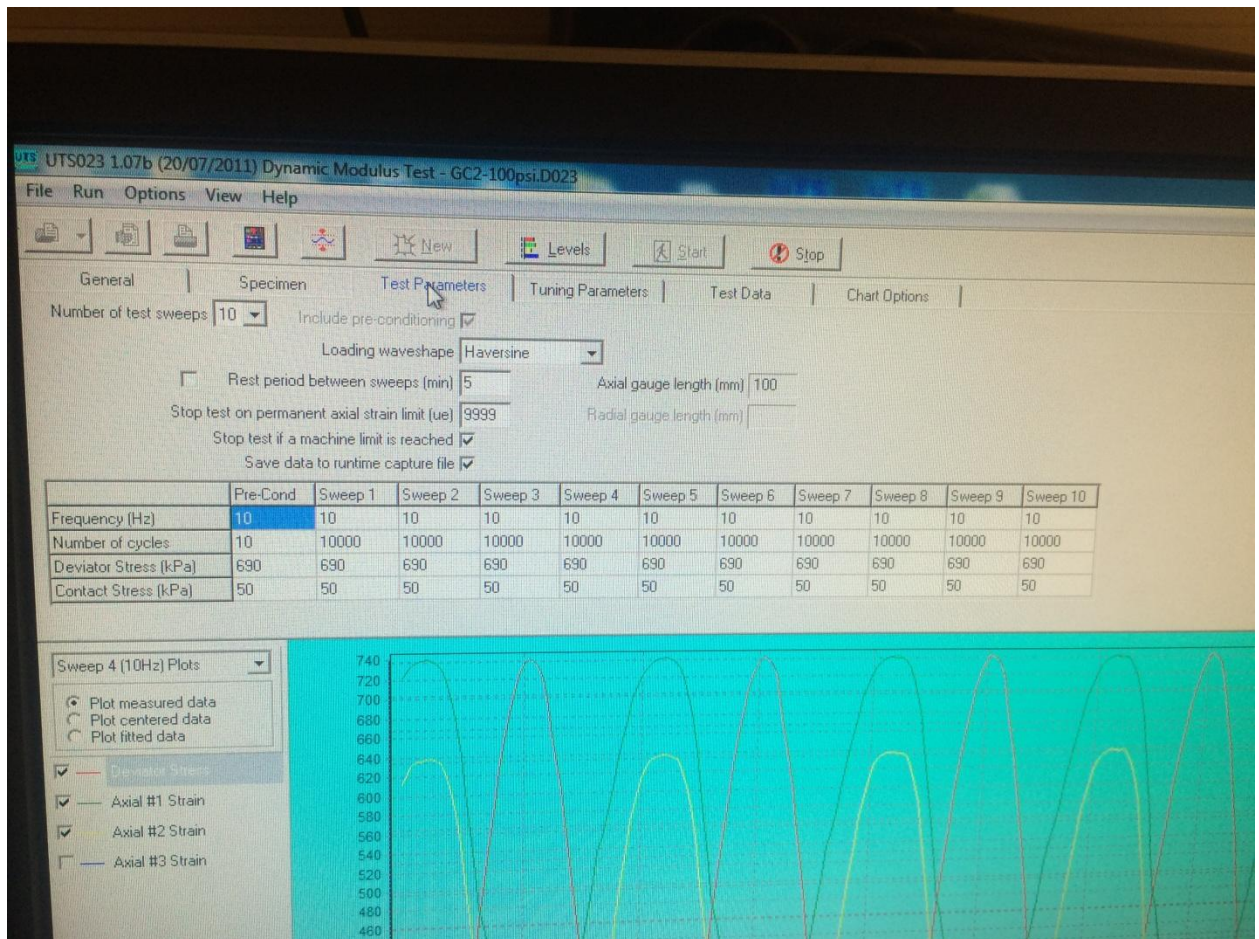
B.3 Dynamic modulus test parameters
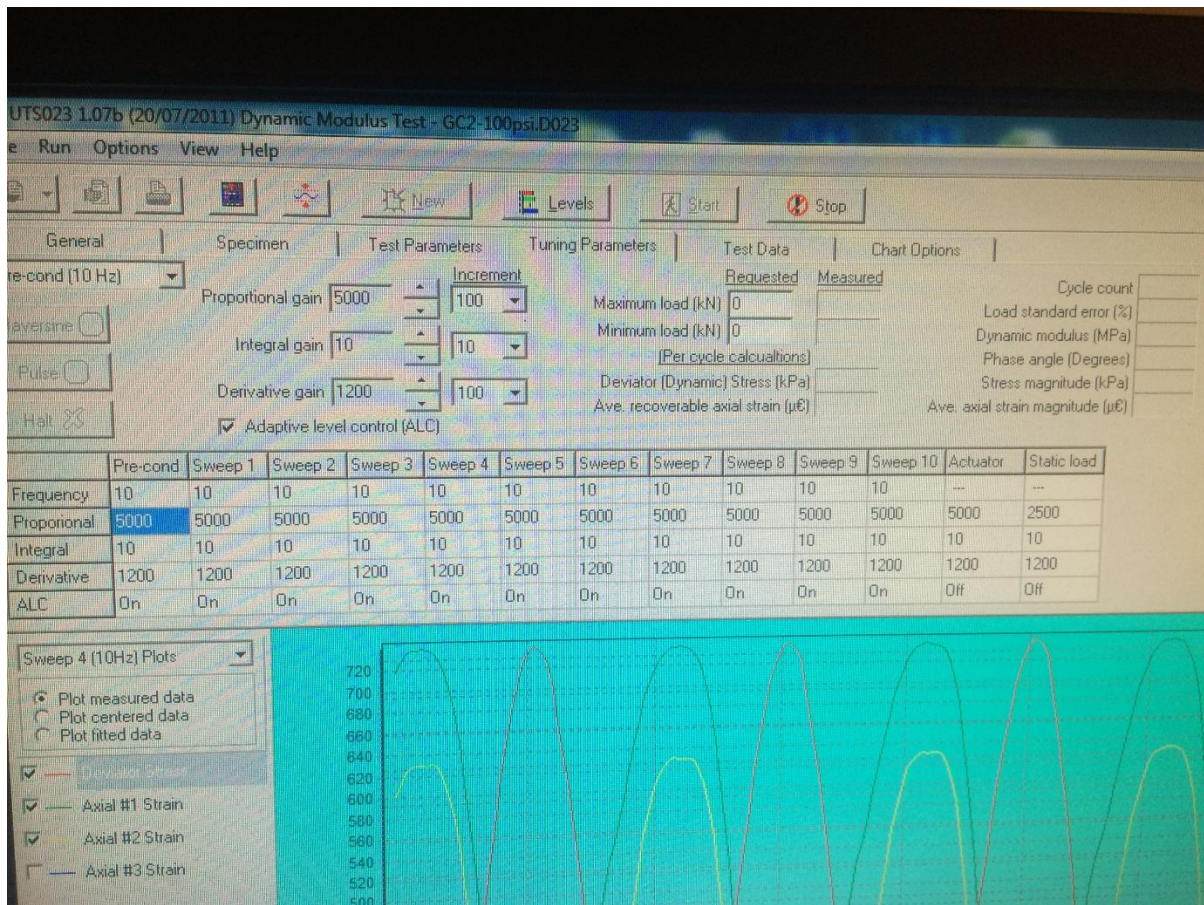
B.4 Dynamic modulus tuning parameters
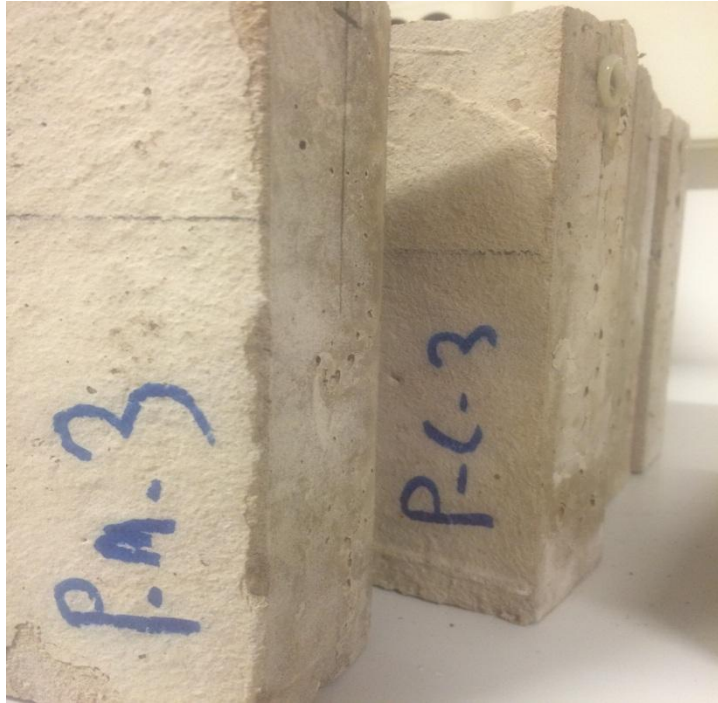
B.6 Failure mechanism photographs
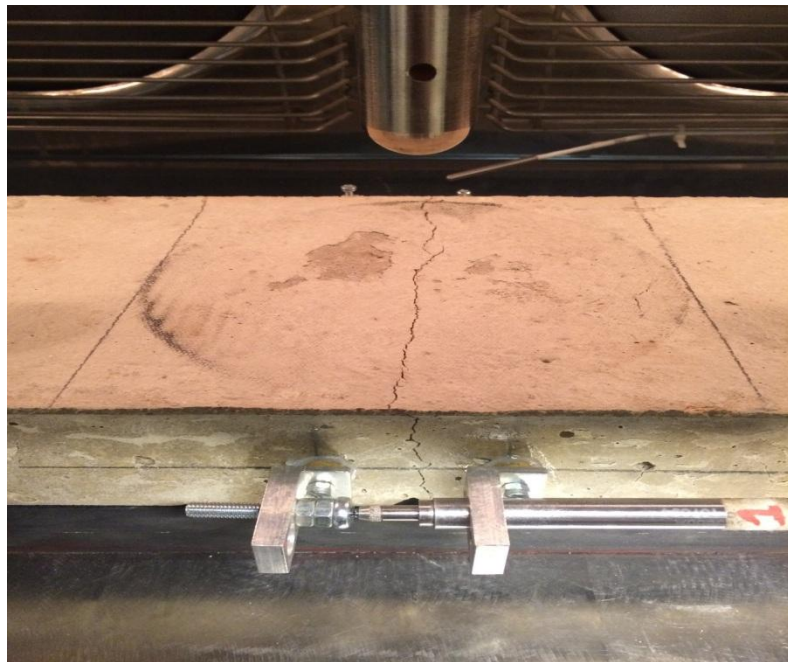
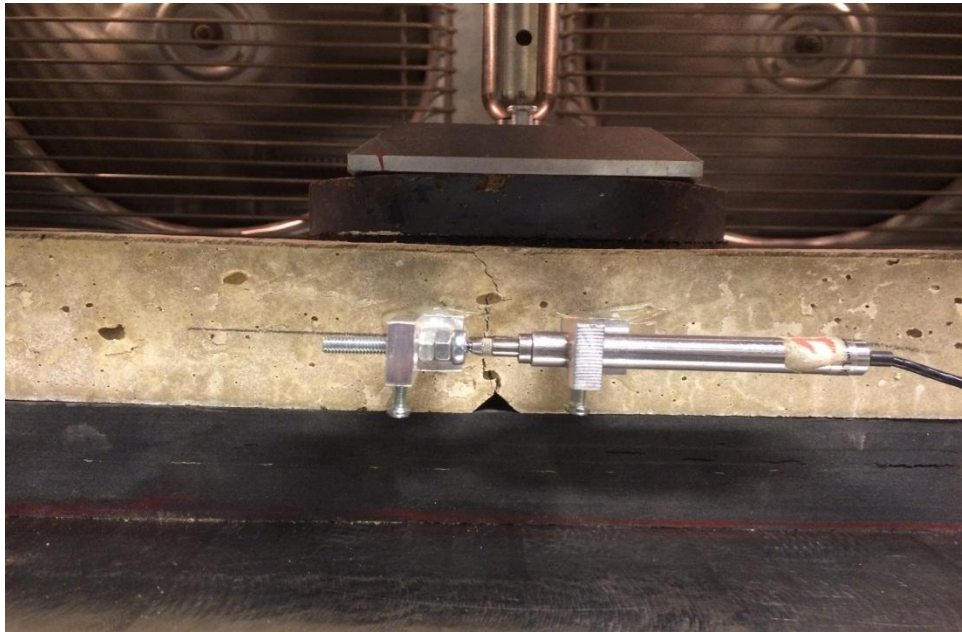*Plain concrete samples*

B.5 Plain concrete sample (P-m-1)

B.6 Plain concrete sample (P-m-2)

B.7 Plain concrete samples (P-m-3 & P-c-3)
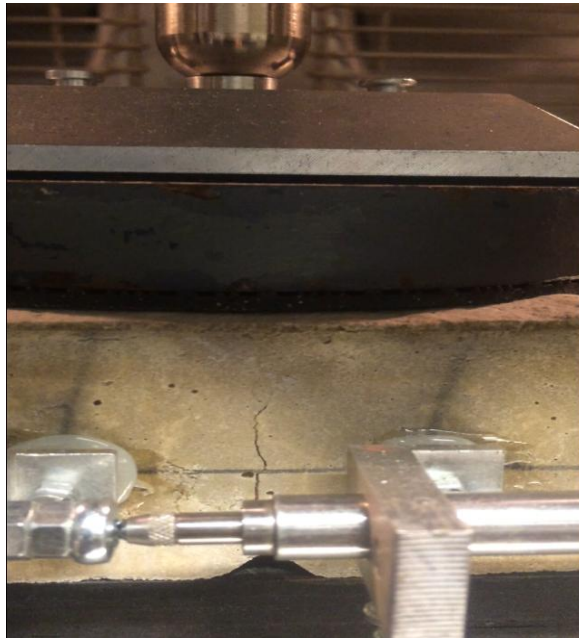

B.8 Plain concrete sample (P-c-1)

B.9 Plain concrete sample (P-c-2)

Geogrid reinforced sample

B.10 Geogrid reinforced sample (G-m-1)

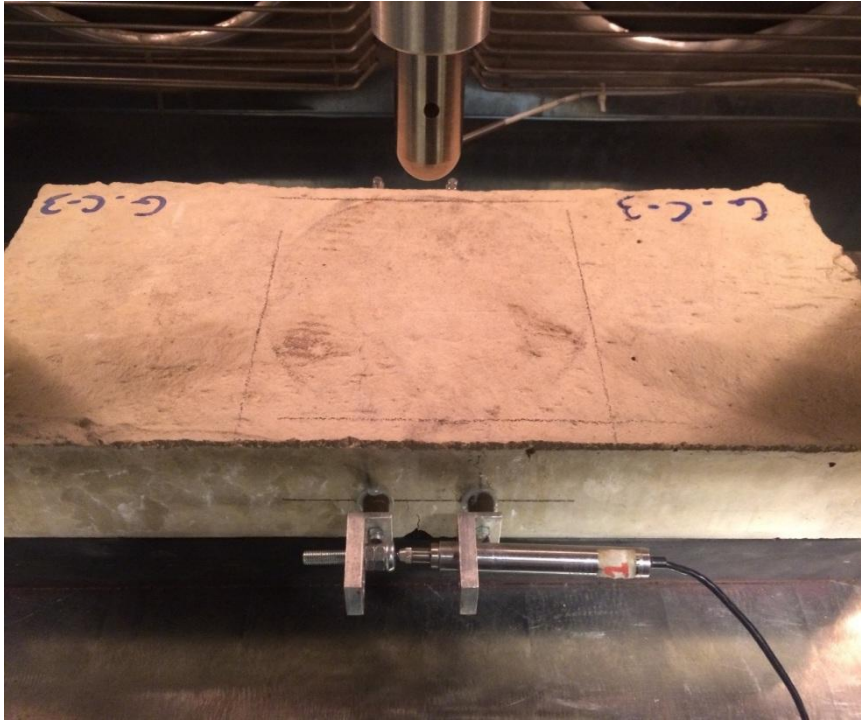B.11 Geogrid reinforced sample (G-m-2)

B.12 Geogrid reinforced sample (G-m-3)

B.13 Geogrid reinforced sample (G-c-1)

B.14 Geogrid reinforced sample (G-c-2)

B.15 Geogrid reinforced sample (G-c-3)